Theoretical background and application of MANSIM for ship maneuvering simulations

Omer Faruk Sukas*, Omer Kemal Kinaci, Sakir Bal

Faculty of Naval Architecture and Ocean Engineering, Istanbul Technical University, TURKEY

**Corresponding author e-mail:* sukaso@itu.edu.tr

Abstract

In this study, a new developed code, MANSIM (MANeuvering SIMulation) for ship maneuvering simulations and its theoretical background are introduced. To investigate the maneuverability of any low-speed ship with single-rudder/single-propeller (SPSR) or twin-rudder/twin-propeller (TPTR) configurations, a 3-DOF modular mathematical model or empirical approaches can be utilized in MANSIM. In addition to certain maneuvers of ships such as turning or zigzag, free maneuver can also be simulated. Input parameters required to solve the equations of motion can be estimated practically by several empirical formulas embedded in the software. Graphical user interface of the code has simple design to enable users to perform maneuvering calculations easily. In addition to results such as advance, transfer, tactical diameters etc. on the user interface, simulation results can also be analyzed graphically; thus it is possible to examine the variation of kinematic parameters during simulation. Using the code, maneuverabilities of a tanker ship (KVLCC2) and a surface combatant (DTMB5415) is investigated and computed results are compared with free running data for validation purpose. MANSIM can be advantageous for parametric studies and it is a valuable tool especially for sensitivity analysis on ship maneuvering. The software is available online at www.mansim.org. The effects of variation of hydrodynamic derivatives and rudder parameters on general maneuvering performance of ships are investigated by performing sensitivity analyses. It is found that linear moment derivatives and rudder parameters are highly effective in maneuvering motion. Another interesting outcome of this study is identification of the significance of third order coupled derivatives for DTMB5415 hull. Effects of linear derivatives on maneuvering indices are also investigated by MANSIM. Results show that there is not a linear relationship between hydrodynamic derivatives and maneuvering indices.

Keywords: hydrodynamic derivatives; DTMB5415; KVLCC2; MMG; sensitivity analysis; hull-rudder interaction

Abbreviations

Ad	Advance	SB	System-Based
CFDB	CFD-Based	SDA	Steady Drift Angle
EMP	Empirical	SPSR	Single Propeller-Single Rudder
FR	Free Running	STD	Steady Turning Diameter
GUI	Graphical User Interface	STS	Steady Turning Speed
LCG	Longitudinal Center of Gravity	SYR	Steady Yaw Rate
MMG	Maneuvering Modelling Group	TD	Tactical Diameter
NR	Number of Rudders	TPTR	Twin Propeller-Twin Rudder
OA	Overshoot Angle	Tr	Transfer

Symbols

A_B	Submerged bow profile area (m^2)	T_P	Thrust of propeller (N)
a_H	Rudder lateral force increase factor $(-)$	u, v	Velocities in x and y axis at midship (m/s)
A_R	Profile area of movable part of mariner rudder (m^2)	u_P	Longitudinal inflow velocity to propeller (m/s)
B	Ship breadth (m)	u_R, v_R	Longitudinal and lateral inflow velocity components to rudder, respectively (m/s)
C_B	Block coefficient $(-)$	U	Ship velocity at midship, $U = \sqrt{u^2 + v^2}\ (m/s)$
c	Rudder chord length (m)	V_A	Initial speed of ship (knots)
d	Ship mean draught (m)	V_T	Steady turning speed (knots)
D_P	Propeller diameter (m)	w_{P0}	Effective wake fraction at propeller position in straight motion $(-)$
f_α	Rudder lift gradient coefficient $(-)$	w_P	Effective wake fraction at propeller position in maneuvering motion $(-)$
F_N	Rudder normal force (N)	x'_H	Non-dimensional longitudinal position of acting point of additional lateral force $(-)$
Fr	Froude number $(-)$	x'_P, y'_P	Non-dimensional longitudinal and lateral position of propeller from midship $(-)$
H	Rudder span (m)	x'_R, y'_R	Non-dimensional longitudinal and lateral coordinate of rudder position, respectively $(-)$
g	Gravity, $g = 9.81\ (m/s^2)$	X_H	Surge force due to hull in x axis (N)

I_z	Yaw moment of inertia around z axis ($kg\ m^2$)	X_R	Surge force due to rudder in x axis (N)
J_z	Added yaw moment of inertia around z axis ($kg\ m^2$)	X_P	Surge force due to propeller in x axis (N)
J_P	Propeller advance ratio ($-$)	Y_H	Sway force due to hull in y axis (N)
k_0, k_1, k_2	Propeller open water characteristics for expressing K_T ($-$)	Y_R	Sway force due to rudder in y axis (N)
K_T	Thrust coefficient ($-$)	α_R	Effective inflow angle to rudder (rad)
l'_R	Flow-straightening coefficient of yaw rate for rudder, $l'_R = l_R/L$ ($-$)	β_P	Geometrical inflow angle to propeller in maneuvering ($-$)
L	Overall length of ship (m)	β_R	Effective drift angle at rudder position (rad)
m	Ship mass ($kg; t$)	β	Ship drift angle (rad)
m_x, m_y	Added mass due to ship motion in x and y directions, respectively (kg)	γ_R	Flow-straightening coefficient of sway velocity for rudder ($-$)
n_P	Propeller revolution ($1/s$)	δ	Rudder angle (rad)
N_H	Yaw moment due to hull around z axis ($N\ m$)	ε	Ratio of effective wake fraction in way of propeller and rudder (–)
N_R	Yaw moment due to rudder around z axis ($N\ m$)	η	Ratio of propeller diameter to rudder span ($-$)
$o_0 - x_0y_0z_0$	Earth-fixed coordinate system	κ	An experimental constant for expressing u_R ($-$)
$o - xyz$	Ship-fixed coordinate system	Λ	Rudder aspect ratio ($-$)
r	Yaw rate around z axis at midship (rad/s)	ρ	Water density (kg/m^3)
S	Wetted surface area of ship (m^2)	τ	Static Trim (m)
t_P	Propeller thrust deduction factor in maneuvering motions ($-$)	ψ	Ship heading angle (rad)
t_R	Steering resistance deduction factor ($-$)		

1 Introduction

Predicting maneuverability of ships is considered as one of the most challenging topics in ship hydrodynamics. Maneuvering simulations are generally conducted by using CFD-based or system-based (SB) methods. CFD-based method can be defined as a direct simulation of the actual maneuvering motion, including the steering rudder and rotating propeller (Bhushan et al., 2009; Carrica et al., 2013; Broglia et al., 2015; Ohashi et al., 2018; Duman and Bal, 2019). From practical perspective, this approach is not feasible as it requires enourmous computational power to perform full time-domain simulations. On the other hand, SB methods include the solution of equations of

motion for every time step using the previously calculated hydrodynamic derivatives. The latter method is more practical than the former. However, accuracy of these calculations directly depends on selected mathematical model and hydrodynamic derivatives involved (Guo and Zou, 2017; Toxopeus et al., 2018; Sukas et al., 2019). In the recent literature, current trend to express the hydrodynamic forces and moments is adopting either Abkowitz model (Abkowitz, 1964) or MMG model (Ogawa and Kasai, 1978; Yoshimura, 2005; Yasukawa and Yoshimura, 2015). In Abkowitz model; hull, rudder and propeller are considered as one rigid body, and equations of motion are defined by third-order Taylor series function. On contrary to Abkowitz model, MMG model is a simplified mathematical model that decomposes total hydrodynamic force and moment acting on the ship into hull, rudder and propeller components. One of the biggest advantages of MMG model is that it allows to take the hull-rudder-propeller interactions into account. There are various maneuvering simulation results using MMG model with different modified versions (Fang et al., 2005; Kang et al., 2008; He et al., 2016; Yasukawa et al., 2019).

There are several prediction methods proposed in literature to determine the hydrodynamic derivatives in MMG models (Sukas et al., 2017a; Sukas et al., 2017b). For example, Yasukawa and Yoshimura (2015) carried out circular motion tests (CMT) to obtain the hydrodynamic derivatives and it was noted that CMT is a suitable method since it has zero frequency of motion which reduces the uncertainties for hydrodynamic forces and moment. PMM (Planar Motion Mechanism) tests are also widely used to determine the hydrodynamic derivatives (Cura-Hochbaum, 2011; Obreja et al. 2012; Sakamoto et al., 2012; Yoon et al., 2015; Duman and Bal, 2017). Accuracy of results based on the selection of PMM motion frequency and amplitude may even change. However, this issue can be handled if PMM motion parameters are selected properly according to ITTC Recommendations (ITTC 7.5-02-06-02, 2014). Recent study has shown that changing the advancing speed of ship in PMM tests has a significant effect on the hydrodynamic derivatives in MMG model (Zhang et al., 2019). In addition to these methods, Liu et al. (2017) presented an integrated empirical maneuvering model for inland vessels. Furthermore, all hydrodynamic derivatives and propeller/rudder parameters in MMG model were estimated by various regression formulas selected from literature. On the other hand, system identification techniques have also been used for estimation of the hydrodynamic derivatives (Zhang and Zou, 2013; Sutulo and Soares, 2014; Yin et al., 2015; Xu et al., 2019). In order to predict maneuverability of any ship using system-based approach, these methods can be utilized to obtain the hydrodynamic derivatives, propeller/rudder parameters.

In this study, a new user-friendly ship maneuvering code called MANSIM (MANeuvering SIMulation) based on standard MMG mathematical model (Yasukawa and Yoshimura, 2015) is introduced. The code includes several empirical relations suggested by various researchers working on the topic and is for those who would like to have a fundamental background of the maneuvering abilities a ship during early design stages. The primary aim here by developing such a code is to make the maneuvering predictions of ships easier by using a simple user interface. The software allows to simulate the turning and zigzag maneuvers of ships. In addition, a free maneuver option is also available with unlimited number of rudder angles which means one can simulate free maneuver of any ship in MANSIM by importing a .txt file that includes rudder angles with respect to times. MANSIM displays the maneuvering results such as advance distance, transfer distance, tactical diameter etc. Input parameters of the mathematical model, such as hydrodynamic derivatives and coefficients related to the propeller and rudder, can also be estimated by several empirical formulas embedded in the

software. The empirical approach provided by Lyster and Knights (1978) may also be preferred as a second option to have a basic understanding of maneuvering abilities of a ship.

Following this section, section 2 presents the theoretical background of MANSIM including the empirical approach suggested by Lyster and Knights (1978) and MMG models for SPSR and TPTR ships. Section 3 gives the empirical formulas embedded in software to estimate input parameters of MMG model. GUI of code was briefly introduced and sample screenshots were given in Section 4. In section 5, maneuverability of two benchmark ships (KVLCC2 and DTMB5415) was examined for validation purposes and the results predicted were compared with the free running test data. In addition, the effect of variation of hydrodynamic derivatives and rudder parameters on general maneuvering performance was investigated by performing a parametrical sensitivity analysis. Finally, section 6 includes brief summary and possible future studies about MANSIM.

2 Theoretical Background

In MANSIM, maneuvering performance of ships can be predicted by using either the empirical model provided by Lyster and Knights (1979) or the mathematical models presented by Khanfir et al. (2011) and Yasukawa and Yoshimura (2015). Further details are explained in the following sub-sections.

2.1 Empirical Approach

Range (maximum and minimum values) of parameters for ships used by Lyster and Knights (1979) are given in Table 1. Empirical formulations have been derived based on the model experiments.

Table 1. Range of ship parameters used by Lyster and Knights (1979).

	$Single-Propeller\ Ships$		$Twin-Propeller\ Ships$	
$Parameters$	$Min.$	$Max.$	$Min.$	$Max.$
$L_{PP}\ [m]$	54.86	329.18	76.20	225.55
C_B	0.56	0.87	0.42	0.62
δ	10.00	45.00	10.00	35.00
B/L	0.11	0.18	0.06	0.20
τ/L	0.00	0.05	-0.01	0.03
Hc/Ld	0.01	0.04	0.01	0.02
$V_A/\sqrt{L}$	0.20	1.00	0.25	2.20

Turning maneuver indices of SPSR ships can be calculated by the following semi-empirical expressions:

$$\frac{\mathrm{STD}}{\mathrm{L}} = 4.19 - 203\frac{\mathrm{C_B}}{\delta} - 13.0\frac{\mathrm{B}}{\mathrm{L}} + \frac{194}{\delta} - 35.8\frac{\mathrm{Hc}}{\mathrm{Ld}}(\mathrm{ST}-1) + 3.82\frac{\mathrm{Hc}}{\mathrm{Ld}}(\mathrm{ST}-2) + 7.79\frac{\mathrm{A_B}}{\mathrm{Ld}} \tag{1}$$

$$\frac{\mathrm{TD}}{\mathrm{L}} = 0.910\frac{\mathrm{STD}}{\mathrm{L}} + 0.424\frac{V_A}{\sqrt{L}} + 0.675 \tag{2}$$

$$\frac{\mathrm{Ad}}{\mathrm{L}} = 0.519\frac{\mathrm{TD}}{\mathrm{L}} + 1.33 \tag{3}$$

$$\frac{\mathrm{Tr}}{\mathrm{L}} = 0.497\frac{\mathrm{TD}}{\mathrm{L}} - 0.065 \tag{4}$$

$$\frac{\mathrm{V_T}}{\mathrm{V_A}} = 0.074\frac{\mathrm{TD}}{\mathrm{L}} + 0.149 \tag{5}$$

where,

$ST = 1$ if $dc \leq Hc$, $ST = 2$ if $dc > Hc$

For TPTR ships, empirical formulas for turning maneuver indices are given as follows:

$$\frac{\mathrm{STD}}{\mathrm{L}} = 0.727 - 197\frac{\mathrm{C_B}}{\delta} + 4.65\frac{\mathrm{B}}{\mathrm{L}} + \frac{188}{\delta} - 218\frac{\mathrm{Hc}}{\mathrm{Ld}}(\mathrm{NR} - 1) + 1.767\frac{\mathrm{V_A}}{\sqrt{\mathrm{L}}} + 25.56\frac{\mathrm{A_B}}{\mathrm{Ld}} \tag{6}$$

$$\frac{\mathrm{TD}}{\mathrm{L}} = \frac{\mathrm{STD}}{\mathrm{L}} + 0.14 \tag{7}$$

$$\frac{\mathrm{Ad}}{\mathrm{L}} = 0.514\frac{\mathrm{TD}}{\mathrm{L}} + 1.1 \tag{8}$$

$$\frac{\mathrm{Tr}}{\mathrm{L}} = 0.531\frac{\mathrm{TD}}{\mathrm{L}} - 0.357 \tag{9}$$

$$\frac{\mathrm{V_T}}{\mathrm{V_A}} = 0.028\frac{\mathrm{TD}}{\mathrm{L}} + 0.543 \tag{10}$$

Here, Ad, Tr, TD, STD and V_T represent the turning maneuver indices and are advance, transfer, turning diameter, steady turning diameter and steady turning speed, respectively. L, B, d and C_B are the main particulars of ship. A_B is the area of submerged bow profile, τ is the static trim and V_A is the initial approach velocity of the ship. Parameters related to rudder are rudder angle (δ), span length (H), chord length (c) and number of rudders (NR).

2.2 Modular Mathematical Model

In MMG model, hydrodynamic forces and moment acting on the ship are divided into different parts (contributors) such as hull, rudder(s) and propeller(s). Major advantage of this method compared to traditional approach (Abkowitz-type) is including interaction effects of hull-rudder(s) and hull-propeller(s). MANSIM contains certain assumptions due to the implementation of MMG model (Yasukawa and Yoshimura, 2015). These assumptions are given below.

- Hydrodynamic forces and moment acting on the ship treat quasi-steadily.
- Cruise speed of the ship is sufficiently low so that wave-making resistance is ignored.

- Metacentric height (GM) is relatively large, thus effects of roll-coupling are negligible.

In the present version of MANSIM, mathematical models for SPSR (Yasukawa and Yoshimura, 2015) and TPTR (Khanfir et al., 2011) ships are available to predict the maneuvering performance in calm water condition. Following sections present the coordinate system, non-dimensionalization and the mathematical models for SPSR and TPTR ships, respectively.

2.2.1 Coordinate System and Non-Dimensionalization

The basic dynamic of motion is described by using Newton's second law of motion. Thus, two different coordinate systems can be defined for a maneuvering ship: earth-fixed coordinate system ($O - X_0Y_0Z_0$) and ship-fixed ($o - xyz$) coordinate system as shown in Figure 1.

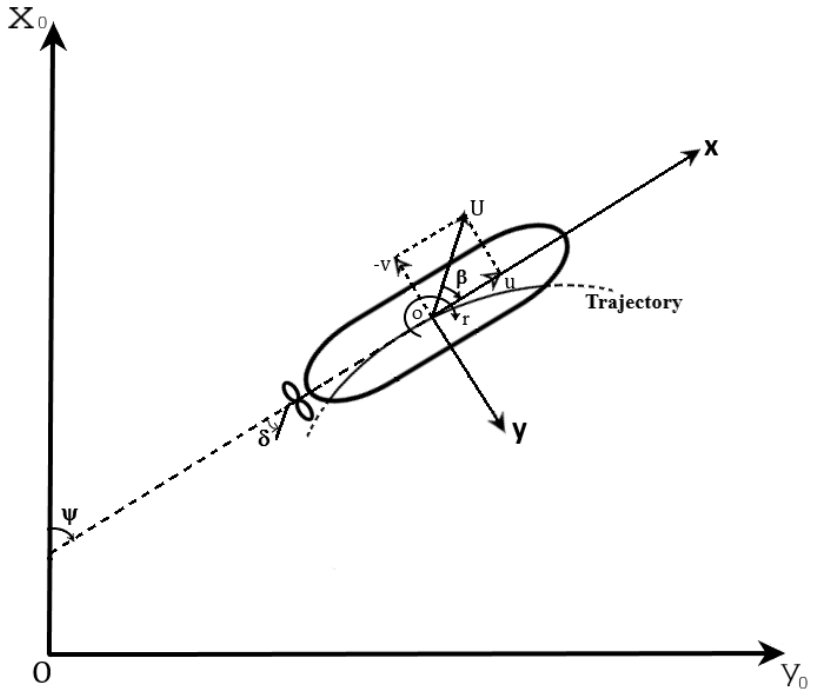

Figure 1. Coordinate system used in calm water.

Here heading angle ψ refers to angle between x and x_0 axis. The difference between ship's heading and actual course direction (velocity vector at COG) is drift angle, $\beta = \tan^{-1}(-v/u)$. The rudder angle, δ is positive while rotating to starboard side. u and v denote velocity components in x and y directions, respectively. r is the yaw rate that can also be defined as $r = \frac{\partial \psi}{\partial t}$. The speed of ship is indicated as $U\ (= \sqrt{u^2 + (-v)^2})$.

In MANSIM, hydrodynamic forces and moment, mass, added mass, moment of inertia, added moment of inertia and other kinematical parameters are non-dimensionalized as given in Table 2.

Table 2. Non-dimensionalization of ship and kinematical parameters.

Parameters	Non-dimensionalized by
X, Y	$^1/_2\,\rho U^2 L d$
N	$^1/_2\,\rho U^2 L^2 d$
u, v	U
r	U/L

m, m_x, m_y	$1/2\,\rho L^2 d$
I_z, J_z	$1/2\,\rho L^4 d$

2.2.2 Mathematical Model

Maneuverability of only low-speed ships in the horizontal plane with sufficiently large GM is considered in the mathematical model of MANSIM. Ship motions withn six degree-of-freedom (6-DOF) were reduced to 3-DOF under the following assumptions:

- Vertical motions (heave, pitch and roll) are ignored. Then $w = p = q = \dot{w} = \dot{p} = \dot{q} = 0$.
- Ship was assumed to have symmetry over xz plane, then $y_G = 0$.

In this case, 3-DOF motion equations become:

$$\begin{aligned} m[\dot{u} - rv - x_G r^2] &= F_x \\ m[\dot{v} + ur + x_G \dot{r}] &= F_y \\ I_{zG}\dot{r} + m x_G(\dot{v} + ur) &= N_z \end{aligned} \tag{11}$$

Forces and moments on the right-hand sides of these equations can be written separately:

$$\begin{aligned} F_x &= -m_x \dot{u} + m_y vr + X \\ F_y &= -m_y \dot{v} - m_x ur + Y \\ N_z &= -J_z \dot{r} + N - x_G F_y \end{aligned} \tag{12}$$

3-DOF motion equations then become;

$$\begin{aligned} (m + m_x)\dot{u} - (m + m_y)vr - x_G m r^2 &= X \\ (m + m_y)\dot{v} + (m + m_x)ur + x_G m \dot{r} &= Y \\ (I_{zG} + {x_G}^2 m + J_z)\dot{r} + x_G m(\dot{v} + ur) &= N \end{aligned} \tag{13}$$

X, Y and N can be divided into sub-components due to the modular structure of MMG model:

$$\begin{aligned} X &= X_H + X_R + X_P \\ Y &= Y_H + Y_R \\ N &= N_H + N_R \end{aligned} \tag{14}$$

where the subscripts H, R and P refer to hull, rudder and propeller, respectively. 3-DOF motion equations can be written in matrix form as follows,

$$Acc = M^{-1} \cdot (P - C \cdot Vel) \tag{15}$$

where Acc matrix includes acceleration terms ($Acc = [\dot{u} \quad \dot{v} \quad \dot{r}]^T$), P forces and moments ($P = [X_H + X_R + X_P \quad Y_H + Y_R \quad N_H + N_R]^T$) and Vel the velocity terms ($Vel = [u \quad v \quad r]^T$). M^{-1} is the inverse of mass matrix and C is the Coriolis matrix. Mass matrix M and Coriolis matrix C are given as follows:

$$M = \begin{bmatrix} m + m_x & 0 & 0 \\ 0 & m + m_y & x_G m \\ 0 & x_G m & I_{zG} + {x_G}^2 m + J_z \end{bmatrix} \tag{16a}$$

$$C = \begin{bmatrix} 0 & -(m+m_y)r & -x_G mr \\ (m+m_x)r & 0 & 0 \\ x_G mr & 0 & 0 \end{bmatrix} \tag{16b}$$

Using all these matrices, Eqn.15 can be written explicitly as;

$$\begin{bmatrix} \dot{u} \\ \dot{v} \\ \dot{r} \end{bmatrix} = \begin{bmatrix} 1/M_{11} & 0 & 0 \\ 0 & M_{33}/\det M & -M_{32}/\det M \\ 0 & -M_{23}/\det M & M_{22}/\det M \end{bmatrix} \cdot \begin{bmatrix} X_H + X_R + X_P + v(m+m_y) + rx_G mr \\ Y_H + Y_R - (m+m_x)ur \\ N_H + N_R - x_G mur \end{bmatrix} \tag{17}$$

The first equation is solved separately, while the others need to have a coupled solution. Moment of inertia around z axis in the mass matrix M is not given by the user, but assumed as approximately $I_z \cong m(0.25L_{pp})^2$. External forces and moment given in the right-hand side (RHS) of Eqn.13 are explained in the following sub-sections.

2.2.2.1 Hull Forces and Moment

Hydrodynamic forces and moment acting on both SPSR and TPTR hulls are expressed as follows (Yasukawa and Yoshimura, 2015):

$$\begin{aligned} X_H &= -X_0(u) + X_{vv}v^2 + X_{vr}vr + X_{rr}r^2 + X_{vvvv}v^4 \\ Y_H &= Y_v v + Y_r r + Y_{vvv}v^3 + Y_{vvr}v^2 r + Y_{vrr}vr^2 + Y_{rrr}r^3 \\ N_H &= N_v v + N_r r + N_{vvv}v^3 + N_{vvr}v^2 r + N_{vrr}vr^2 + N_{rrr}r^3 \end{aligned} \tag{18}$$

where all coefficients here (X_{vv}, Y_{vvv}, Y_{vrr}, N_{rrr}, etc.) are known as hydrodynamic derivatives or maneuvering coefficients.

2.2.2.2 Propeller Forces and Moment

Propeller surge force (X_P) is calculated for SPSR (Yasukawa and Yoshimura, 2015) and TPTR (Khanfir et al., 2011) ships with the parameters given in Table 3. Note that side force (Y_P) and yaw moment (N_P) due to propeller are neglected as they have smaller magnitudes compared to those of hull and rudder components. The superscripts 'P' and 'S' in Table 3 represent port and starboard propellers, respectively.

Table 3. Hydrodynamic force due to propeller for single and twin propeller ships.

Definition	Single-Propeller Ships	Twin-Propeller Ships
Surge force due to propeller(s)	$X_P = (1-t_P)T_p$	$X_P^{P,S} = (1-t_P^{P,S})T_p^{P,S}$
Thrust of propeller(s)	$T_p = \rho n_P^2 D_P^4 K_T$	$T_p^{P,S} = \rho n_P^2 D_P^4 K_T^{P,S}$
Thrust coefficent	$K_T = k_0 + k_1 J_P + k_2 J_P^2$	$K_T^{P,S} = k_0 + k_1 J_P^{P,S} + k_2 (J_P^{P,S})^2$
Propeller(s) advance ratio	$J_P = \dfrac{u_P}{n_P D_P}$	$J_P^{P,S} = \dfrac{u_P^{P,S}}{n_P D_P^{P,S}}$
Inflow velocity to propeller(s)	$u_P = u(1-w_P)$	$u_P^{P,S} = (1-w_P^{P,S})(u + y_P^{P,S} r)$
Wake fraction of propeller(s)	$w_P = w_{P0}\exp(-4\beta_P^2)$	$w_P^{P,S} = w_{P0}^{P,S}\exp(-4(\beta_P^{P,S})^2)$
Geometrical inflow angle	$\beta_P = \beta - \mathrm{x}'_P r'$	$\beta_P^{P,S} = \beta - (\mathrm{x}'_P)^{P,S} r'$

Here, t_P is propeller thrust deduction factor in maneuvering motion, n_P is propeller rotation rate and D_P is propeller diameter. k_0, k_1 and k_2 represent open water characteristics of propeller for expressing K_T. w_{P0} denotes the effective wake fraction at propeller position in straight motion and x'_P is non-dimensional longitudinal position of propeller from midship.

2.2.2.3 Rudder Forces and Moment

Forces and moment related to rudder (X_R, Y_R, N_R) for single-rudder ships are calculated based on rudder normal force (F_N), rudder angle (δ) and hull-rudder interaction coefficients (t_R, a_H, x_H) by the following equations (Yasukawa and Yoshimura, 2015):

$$X_R = -(1-t_R)F_N \sin\delta$$
$$Y_R = -(1+a_H)F_N \cos\delta \quad (19)$$
$$N_R = -(x_R + a_H x'_H)F_N \cos\delta$$

where t_R is steering resistance deduction factor. a_H and x'_H are rudder lateral force increase factor and non-dimensional longitudinal position of acting point of a_H from midship, respectively. For twin rudder ships, hydrodynamic forces and moment due to rudders are calculated by (Khanfir et al., 2011):

$$X_R = -(1-t_R)(F_N^P sin\delta^P + F_N^S sin\delta^S)$$
$$Y_R = -(1+a_H)(F_N^P cos\delta^P + F_N^S cos\delta^S) \quad (20)$$
$$N_R = -(x_R + a_H x'_H)(F_N^P cos\delta^P + F_N^S cos\delta^S) + (1-t_R)(y_R^P F_N^P sin\delta^P + y_R^S F_N^S sin\delta^S)$$

Here y_R^P and y_R^S are the offsets of rudders from the ship's centerline. Parameters required for prediction of rudder normal force(s) (F_N) during maneuver are given in Table 4.

Table 4. Rudder parameters required to calculate rudder normal force(s).

Definition	Single-Rudder Ships	Twin-Rudder Ships
Rudder normal force	$F_N = 0.5\rho A_R U_R^2 f_\alpha \sin\alpha_R$	$F_N^{P,S} = 0.5\rho A_R^{P,S} (U_R^{P,S})^2 f_\alpha^{P,S} \sin\alpha_R^{P,S}$
Rudder lift gradient coefficient	$f_\alpha = \frac{6.13\Lambda}{\Lambda + 2.25}$	$f_\alpha^{P,S} = \frac{6.13\Lambda^{P,S}}{\Lambda^{P,S} + 2.25}$
Inflow velocity to rudders	$U_R = \sqrt{u_R^2 + v_R^2}$	$U_R^{P,S} = \sqrt{(u_R^{P,S})^2 + (v_R^{P,S})^2}$
Effective inflow angle to rudder(s)	$\alpha_R = \delta - \tan^{-1}(\frac{v_R}{u_R})$	$\alpha_R^{P,S} = \delta^{P,S} - (\gamma_R^{P,S}\beta_R^{P,S} - \tan^{-1}(\frac{y_R^{P,S}}{x_P^{P,S}}))$
Effective inflow angle to rudder(s) in maneuvering	$\beta_R = \beta - l'_R r'$	$\beta_R^{P,S} = \beta - (l'_R)^{P,S} r'$

Longitudinal inflow velocity to rudder(s)	$u_R = \varepsilon u_P \sqrt{\eta\left\{1+\kappa\left(\sqrt{1+\frac{8K_T}{\pi J_P^2}}-1\right)\right\}^2+(1-\eta)}$	$u_R^{P,S} = \varepsilon^{P,S} u_P^{P,S} \sqrt{\eta\left\{1+\kappa^{P,S}\left(\sqrt{1+\frac{8K_T^{P,S}}{\pi (J_p^{P,S})^2}}-1\right)\right\}^2+(1-\eta)}$
Lateral inflow velocity to rudder(s)	$v_R = \gamma_R \beta_R$	$v_R^{P,S} = u_R^{P,S}\tan(\gamma_R^{P,S}\beta_R^{P,S} - \tan^{-1}(\frac{y_R^{P,S}}{x_P^{P,S}}))$

Here, ε, κ, l_R and γ_R are unknown rudder parameters that need to be estimated empirically, numerically or experimentally. A_R is the profile area of movable part of rudder, Λ is aspect ratio of rudder and η is ratio of propeller diameter to rudder span. Note that equation provided for rudder lift gradient coefficient (f_α) is suggested by Fujii and Tuda (1961).

3 Empirical Equations

All input parameters should be inserted to obtain full maneuvering performance of a ship in MANSIM. In case no input data is available for hydrodynamic parameters of hull, rudder and propeller; empirical relations embedded in MANSIM can be applied. These empirical equations are taken from various studies in related literature. From practical point of view, empirical formulas may be useful to assess the order of magnitudes of parameters in the preliminary design stage. The empirical formulas embedded in MANSIM are given in the following sub-sections.

3.1 Added Mass and Added Moment of Inertia

Empirical formulas embedded in software for the estimation of added masses m_x, m_Y and added moment of inertia J_Z are given in Table 5. All formulas provided are based on the main particulars of ship such as; m, L, B, d and C_B. It should be noted that m_x is advised to be taken approximately as $3-6\%$ of ship mass (m) in Clarke et. al. (1983), where it is taken as 5% of ship mass in MANSIM.

Table 5. Empirical relations to estimate m_x, m_Y and J_Z.

Reference	Empirical Formula
Clarke et. al. (1983)	$m_x = m * 0.05$
Zhou et. al. (1983)	$m_Y = m\left[0.882 - 0.54C_B\left(1-1.6\frac{d}{B}\right) - 0.156(1-0.673C_B)\frac{L}{B} + 0.826\frac{d}{B}\frac{L}{B}\left(1-0{,}678\frac{d}{B}\right) - 0.638C_B\frac{d}{B}\frac{L}{B}\left(1-0.669\frac{d}{B}\right)\right]$
Zhou et. al. (1983)	$J_Z = m\left[\frac{1}{100}\left(33 - 76.85C_B(1-0.784C_B) + 3.43\frac{L}{B}(1-0.63C_B)\right)\right]^2$

3.2 Hydrodynamic Derivatives

In this section, the empirical formulas existed in the software to estimate the hydrodynamic derivatives are presented. Table 6, Table 7 and Table 8 show the empirical formulas provided for derivatives related to surge force (X), sway force (Y) and yaw moment (N), respectively. Total resistance coefficient (X_0') is calculated by Holtrop method (Holtrop, 1978). Note that the accuracy of empirical

relations may change with range of ship parameters and mathematical model used in the corresponding study. Note that all empirical equations given in Tables 6-8 have been rearranged according to non-dimensionalization procedure used in MANSIM.

Table 6. Empirical formulas for hydrodynamic derivatives for surge force (X).

Reference	Empirical Formula
Lee et. al. (1998)	$X_{VV} = 0.0014 - 0.1975d\frac{(1-C_B)}{B}\frac{L}{d}$
Yoshimura and Masumoto (2012)	$X_{VV} = 1.15\frac{C_B}{L/B} - 0.18$
Yoshimura and Masumoto (2012)	$X_{VVVV} = -6.68\frac{C_B}{L/B} + 1.1$
Lee et. al. (1998)	$X_{rr} = \left(-0.0027 + 0.0076C_B\frac{d}{B}\right)\frac{L}{d}$
Yoshimura and Masumoto (2012)	$X_{rr} = -0.085\frac{C_B}{L/B} + 0.008 - x_G m_y$
Lee et. al. (1998)	$X_{vr} = \left[m + 0.1176m_y(0.5 + C_B)\right]\frac{L}{d}$
Yoshimura and Masumoto (2012)	$X_{vr} = m_y - 1.91\frac{C_B}{L/B} + 0.08$

Table 7. Empirical formulas for hydrodynamic derivatives for sway force (Y).

Reference	Empirical Formula
Kijima et. al. (1990)	$Y_v = -\left(0.5\pi\frac{2d}{L} + 1.4C_B\frac{B}{L}\right)$
Lee et. al. (1998)	$Y_v = \left(-0.4545\frac{d}{L} + 0.065C_B\frac{B}{L}\right)\frac{L}{d}$
Yoshimura and Masumoto (2012)	$Y_v = -\left(0.5\pi\frac{2d}{L} + 1.4\frac{C_B}{L/B}\right)$
Clarke et. al. (1983)	$Y_v = \left[-\pi\left(\frac{d}{L}\right)^2(1 + 0.4C_B\frac{B}{d})\right]\frac{L}{d}$
Smitt (1970)	$Y_v = -\pi\left(\frac{d}{L}\right)^2 1.59\ \frac{L}{d}$
Norrbin (1971)	$Y_v = \left[-\pi\left(\frac{d}{L}\right)^2(1.69 + 0.08\frac{C_B}{\pi}\frac{B}{d})\right]\frac{L}{d}$
Inoue et. al. (1981)	$Y_v = \left[-\pi\left(\frac{d}{L}\right)^2(1 + \frac{1.4}{\pi}C_B\frac{B}{d})\right]\frac{L}{d}$
Khattab (1984)	$Y_v = \left[-\pi\left(\frac{d}{L}\right)^2(\frac{2.3}{\pi} + \frac{1.466}{\pi}C_B\frac{B}{d} - \frac{0.00102}{\pi}\left(\frac{L}{d}\right)^2\right]\frac{L}{d}$
Ankudinov (1987)	$Y_v = \left[-\pi\left(\frac{d}{L}\right)^2 K_y(0.25(C_B\frac{B}{d})^2 - 1.5C_B\frac{B}{d} + 3.45)\right]\frac{L}{d}$ $if \quad C_B\frac{B}{d} > 5 \qquad K_y = 5\frac{d}{C_B B}\ ;\ else\ \ K_y = 1$
Lee et. al. (1998)	$Y_{vvv} = \left(-0.6469(1-C_B)\frac{d}{B} + 0.0027\right)\frac{L}{d}$

Yoshimura and Masumoto (2012)	$Y_{vvv} = -0.185\frac{L}{B} + 0.48$
Kijima et. al. (1990)	$Y_r = (m + m_x) - 1.5C_B\frac{B}{L}$
Lee et. al. (1998)	$Y_r = \left(-0.115C_B\frac{B}{L} + 0.0024\right)\frac{L}{d}$
Yoshimura and Masumoto (2012)	$Y_r = m_x + 0.5C_B\frac{B}{L}$
Clarke et. al. (1983)	$Y_r = \left[-\pi\left(\frac{d}{L}\right)^2(-0.5 + 2.2\frac{B}{L} - 0.080\frac{B}{d})\right]\frac{L}{d}$
Smitt (1970)	$Y_r = \left[-\pi\left(\frac{d}{L}\right)^2(-0.32)\right]\frac{L}{d}$
Norrbin (1971)	$Y_r = \left[-\pi\left(\frac{d}{L}\right)^2(-0.645 + 0.38\frac{C_B}{\pi}\frac{B}{d})\right]\frac{L}{d}$
Inoue et. al. (1981)	$Y_r = \left[(-0.5)\left(-\pi\left(\frac{d}{L}\right)^2\right)\right]\frac{L}{d}$
Khattab (1984)	$Y_r = \left[-\pi\left(\frac{d}{L}\right)^2(\frac{-1.0328}{\pi} - \frac{0.11}{\pi}C_B\frac{B}{d} - \frac{0.00004}{\pi}\left(\frac{L}{d}\right)^2\right]\frac{L}{d}$
Ankudinov (1987)	$Y_r = \left[-\pi\left(\frac{d}{L}\right)^2\left(-\left(0.3 - C_B\frac{B}{L}\right)Y_v\left(-\pi\left(\frac{d}{L}\right)^2\right)\right)\right]\frac{L}{d}$
Lee et. al. (1998)	$Y_{rrr} = \left[-0.0233C_B\frac{d}{B} + 0.0063\right]\frac{L}{d}$
Yoshimura and Masumoto (2012)	$Y_{rrr} = -0.051$
Kijima et. al. (1990)	$Y_{vrr} = -\left[5.95d\frac{(1 - C_B)}{B}\right]$
Lee et. al. (1998)	$Y_{vrr} = -\left[0.4346(1 - C_B)\frac{d}{B}\right]\frac{L}{d}$
Yoshimura and Masumoto (2012)	$Y_{vrr} = -\left[0.26(1 - C_B)\frac{L}{B} + 0.11\right]$
Kijima et. al. (1990)	$Y_{vvr} = 1.5d\frac{C_B}{B} - 0.65$
Lee et. al. (1998)	$Y_{vvr} = \left(0.1234C_B\frac{d}{B} - 0.001452\right)\frac{L}{d}$
Yoshimura and Masumoto (2012)	$Y_{vvr} = -0.75$

Table 8. Empirical formulas for hydrodynamic derivatives for yaw moment (N).

Reference	Empirical Formula
Kijima et. al. (1990)	$N_v = -2\frac{d}{L}$
Lee et. al. (1998)	$N_v = (-0{,}23\frac{d}{L} + 0{,}0059)\ \frac{L}{d}$

Yoshimura and Masumoto (2012)

$$N_v = -2\frac{d}{L}$$

Clarke et. al. (1983)

$$N_v = \left(-\pi\left(\frac{d}{L}\right)^2\left(0.5 + 2.4\frac{d}{L}\right)\right)\frac{L}{d}$$

Smitt (1970)

$$N_v = \left(-\pi\left(\frac{d}{L}\right)^2 0.62\right)\frac{L}{d}$$

Norrbin (1971)

$$N_v = \left(-\pi\left(\frac{d}{L}\right)^2\left(0.64 - 0.04\frac{C_B}{\pi}\frac{B}{d}\right)\right)\frac{L}{d}$$

Inoue et. al. (1981)

$$N_v = \left(-\pi\left(\frac{d}{L}\right)^2\frac{2}{\pi}\right)\frac{L}{d}$$

Khattab (1984)

$$N_v = \left[-\pi\left(\frac{d}{L}\right)^2\left(\frac{1.758}{\pi} - \frac{0.00768}{\pi}\frac{C_B L^2}{Bd} - \frac{0.0008}{\pi}\left(\frac{L}{d}\right)^2\right)\right]\frac{L}{d}$$

Ankudinov (1987)

$$N_v = \left[-\pi\left(\frac{d}{L}\right)^2\left(0.75 - 0.04\frac{C_B}{\pi}\frac{B}{d}\right)\right]\frac{L}{d}$$

Lee et. al. (1998)

$$N_{vvv} = \left[0.0348 - 0.5283(1 - C_B)\frac{d}{B}\right]\frac{L}{d}$$

Yoshimura and Masumoto (2012)

$$N_{vvv} = -[-0.69C_B + 0.66]$$

Kijima et. al. (1990)

$$N_r = -0.54\frac{2d}{L} + \left(\frac{2d}{L}\right)^2$$

Lee et. al. (1998)

$$N_r = \left[-0.003724 + 0.10446\frac{d}{L} - 1.393\left(\frac{d}{L}\right)^2\right]\frac{L}{d}$$

Yoshimura and Masumoto (2012)

$$N_r = -0.54\frac{2d}{L} + \left(\frac{2d}{L}\right)^2$$

Clarke et. al. (1983)

$$N_r = \left[-\pi\left(\frac{d}{L}\right)^2\left(0.25 + 0.039\frac{B}{d} - 0.56\frac{B}{L}\right)\right]\frac{L}{d}$$

Smitt (1970)

$$N_r = \left[-0.21\pi\left(\frac{d}{L}\right)^2\right]\frac{L}{d}$$

Norrbin (1971)

$$N_r = \left[-\pi\left(\frac{d}{L}\right)^2\left(0.47 - 0.18\frac{C_B}{\pi}\frac{B}{d}\right)\right]\frac{L}{d}$$

Inoue et. al. (1981)

$$N_r = \left[-\pi\left(\frac{d}{L}\right)^2\left(\frac{1.04}{\pi} - \frac{4}{\pi}\frac{d}{L}\right)\right]\frac{L}{d}$$

Khattab (1984)

$$N_r = \left[-\pi\left(\frac{d}{L}\right)^2\left(\frac{1.3192}{\pi} - 0.68228\frac{C_B}{\pi} - \frac{0.00019}{\pi}\left(\frac{L}{d}\right)^2\right)\right]\frac{L}{d}$$

Ankudinov (1987)

$$N_r = \left[-\pi\left(\frac{d}{L}\right)^2 K_y(0.03(C_B\frac{B}{d})^2 - 0.15C_B\frac{B}{d} + 0.5)\right]\frac{L}{d}$$

$$if \quad C_B\frac{B}{d} > 5 \qquad K_y = 5\frac{d}{C_B B}\ ;\ else\ \ K_y = 1$$

Lee et. al. (1998)

$$N_{rrr} = \left[-0.0572 + 0.03C_B\frac{d}{L}\right]\frac{L}{d}$$

Yoshimura and Masumoto (2012)

$$N_{rrr} = \left[\frac{0.25C_B}{L/B}\right] - 0.056$$

Kijima et. al. (1990)

$$N_{vrr} = \left[0.5d\frac{C_B}{B}\right] - 0.05$$

Lee et. al. (1998)

$$N_{vrr} = \left[-0.0005 + 0.00594C_B\frac{d}{B}\right]\frac{L}{d}$$

Yoshimura and Masumoto (2012)	$N_{vrr} = -0.075(1 - C_B)\frac{L}{B} - 0.098$
Kijima et. al. (1990)	$N_{vvr} = -\left[57.5\left(C_B\frac{B}{L}\right)^2 - 18.4\left(C_B\frac{B}{L}\right) + 1.6\right]$
Lee et. al. (1998)	$N_{vvr} = \left[-1.722 + 22.997\left(C_B\frac{B}{L}\right) - 77.268\left(C_B\frac{B}{L}\right)^2\right]\frac{L}{d}$
Yoshimura and Masumoto (2012)	$N_{vvr} = \left[\frac{1.55C_B}{L/B} - 0.76\right]$

3.3 Self-Propulsion Parameters

Empirical relations used to estimate wake fraction coefficient in straight motion (w_{P0}) and thrust deduction factor (t_P) are given in Table 9 and Table 10, respectively. Empirical equations provided for self-propulsion parameters are based on the main particulars of ship and propeller such as L, B, C_B and D_P. Apart from these parameters, open water characteristics of the propeller (k_0, k_1, k_2) and the propeller revolution (n_P) must be known. Self-propulsion parameters given in MMG model can also be obtained by traditional engineering approach as explained in Kinaci et al. (2018).

Table 9. Empirical formulas for wake fraction coefficient in straight motion, w_{P0}.

Reference	Empirical Formula
Kijima et. al. (1990)	$w_{P0} = 0.5C_B - 0.05$
Harvald (1983)	$w_{P0} = w_1 + w_2 + w_3$ $w_1 = a + \frac{b}{c(0.98 - C_B)^3 + 1}$ $w_2 = -\frac{0.05}{100(C_B - 0.7)^2 + 1}$ $w_3 = -0.18 + \frac{0.00756}{\frac{D_P}{L} + 0.002}$ $a = 0.1\frac{B}{L} + 0.149;\ b = 0.05\frac{B}{L} + 0.449;\ c = 585 - 5027\frac{B}{L} + 11700\left(\frac{B}{L}\right)^2$

Table 10. Empirical formulas for thrust deduction factor, t_P.

Reference	Empirical Formula
Kulzyk (1995)	$t_P = -0.27$
Harvald (1983)	$t_P = t_1 + t_2 + t_3$ $t_1 = d_1 + \frac{e_1}{f_1(0.98 - C_B)^3 + 1}$ $t_2 = 0.02$ $t_3 = 2\left(\frac{D_P}{L} - 0.04\right)$

$$d_1 = 0.625\frac{B}{L} + 0.08$$

$$e_1 = 0.165 - \left(0.25\frac{B}{L}\right)$$

$$f_1 = 525 - 8060\frac{B}{L} + 20300\left(\frac{B}{L}\right)^2$$

3.4 Rudder Parameters

Empirical relations embedded in MANSIM for estimation of hull-rudder interaction coefficients (t_R, a_H, x'_H) are given in Tables 11-13. Here, t_R is the deduction factor of rudder resistance due to existence of ship hull, a_H denotes the factor of lateral force acting on the hull during steering and x'_H represents the application point of this lateral force component in longitudinal direction during steering. Empirical formulas for rudder force parameters are based on the main particulars of ship such as L, B, d, C_B. Alongside of hull-rudder interaction coefficients, there are some necessary coefficients ($\varepsilon, \kappa, l'_R, \gamma$) to be known according to MMG model to predict rudder normal force (F_N). Empirical relations for these coefficients given in related literature are presented in Tables 14-17.

Table 11. Empirical formulations embedded in MANSIM for estimating a_H.

Reference	Empirical Formula
Aoki et. al. (2006)	$a_H = 3.349{C_B}^2 - 3.293C_B + 1.059$
Lee et. al. (1998)	$a_H = 2.78C_B - 1.922$
Yoshimura and Masumoto (2012)	$a_H = 3.6C_B\frac{B}{L}$
Quadvlieg (2013)	$a_H = 0.627C_B - 0.153$
Lee and Shin (1998)	$a_H = -11.4036 + 40.94C_B - 81.11\frac{2d}{L} - 31.69{C_B}^2 + 90.76\left(\frac{2d}{L}\right)^2 + 79.47C_B\frac{2d}{L}$

Table 12. Empirical formulations embedded in MANSIM for estimating x'_H.

Reference	Empirical Formula
Aoki et. al. (2006)	$x'_H = -0.45$
Lee et. al. (1998)	$x'_H = 1.68C_B - 1.968 + 0.5$
Yoshimura and Masumoto (2012)	$x'_H = -0.4$
Lee and Shin (1998)	$x'_H = -6.054 + 58.18\frac{B}{L} - 148.44\left(\frac{B}{L}\right)^2$

Table 13. Empirical formulations embedded in MANSIM for estimating t_R.

Reference	Empirical Formula
Aoki et. al. (2006)	$t_R = -0.629{C_B}^2 + 0.605C_B + 0.129$
Kijima (1990); Lee et. al. (1998)	$t_R = 0.45 - 0.28C_B$
Yoshimura and Masumoto (2012)	$t_R = 0.39$

Table 14. Empirical formulations embedded in MANSIM for estimating ε.

Reference	Empirical Formula
Kijima (1990)	$\varepsilon = -156.2\left(C_B\frac{B}{L}\right)^2 + 41.6\left(C_B\frac{B}{L}\right) - 1.76$
Lee and Shin (1998)	$\varepsilon = -2.3281 + 8.697C_B - 3.78\frac{2d}{L} + 1.19{C_B}^2 + 292\left(\frac{2d}{L}\right)^2 - 82.51C_B\frac{2d}{L}$
Yoshimura and Masumoto (2012)	$\varepsilon = 2.26 * 1.82(1 - w_{P0})$

Table 15. Empirical formulations embedded in MANSIM for estimating κ.

Reference	Empirical Formula
Lee and Shin (1998)	$\kappa = 0.6/(-2.3281 + 8.697C_B - 3.78\,2d/L + 1.19{C_B}^2 + 292(2d/L)^2 - 82.51C_B\,2d/L)$
Yoshimura and Masumoto (2012)	$\kappa = 0.55/(2.26 * 1.82(1 - w_{P0}))$
Yoshimura and Ma (2003)	$\kappa = 0.55 - 0.8C_B\,B/L$

Table 16. Empirical formulations embedded in MANSIM for estimating l'_R.

Reference	Empirical Formula
Kijima et. al. (1990)	$l'_R = 2x_R$
Lee et. al. (1998)	$l'_R = 2x_R$
Yoshimura and Masumoto (2012)	$l'_R = -0.9$
Yoshimura and Ma (2003)	$l'_R = 1.7C_B\frac{B}{L} - 1.2$

Table 17. Empirical formulations embedded in MANSIM for estimating γ_R.

Reference	Empirical Formula
Kijima et. al. (1990)	$\gamma_R = -22.2\left(C_B\frac{B}{L}\right)^2 + 0.02\left(C_B\frac{B}{L}\right) + 0.68$

Lee et. al. (1998)	$\gamma_R = 2.7236 C_B \frac{B}{L} + 0.021$
Yoshimura and Masumoto (2012)	$\gamma_R = 2.06 C_B \frac{B}{L} + 0.14$
Lee and Shin (1998)	$\gamma_R^+ = 23.708 - 83.84 C_B + 173.72 \left(\frac{2d}{L}\right) + 71.64 C_B^2 + 157 \left(\frac{2d}{L}\right)^2 - 261.11 C_B \left(\frac{2d}{L}\right)$ $\gamma_R^- = 6.8736 - 16.77 C_B + 3.5687 \left(\frac{2d}{L}\right) + 4.68 C_B^2 - 253.14 \left(\frac{2d}{L}\right)^2 + 74.83 C_B \left(\frac{2d}{L}\right)$

4 Graphical User Interface

Graphical user interface (GUI) of MANSIM provides an easy utilization to use mathematical models and empirical approaches, and has been designed to be a practical tool for ship maneuvering simulations. Mathematical models embedded in MANSIM are available for SPSR (Yasukawa and Yoshimura, 2015) and TPTR (Khanfir et al., 2011) ships to simulate turning, zigzag and free maneuvers in calm water. Mathematical models for SPSR and TPTR ships were explained in detail in Section 2.2. In addition to mathematical models, turning maneuver of single-propeller and twin-propeller ships can be predicted based on the empirical relations provided by Lyster and Knights (1979). Details of this approach are given in Section 2.1. A flow diagramme of GUI of MANSIM is shown in Figure 2.

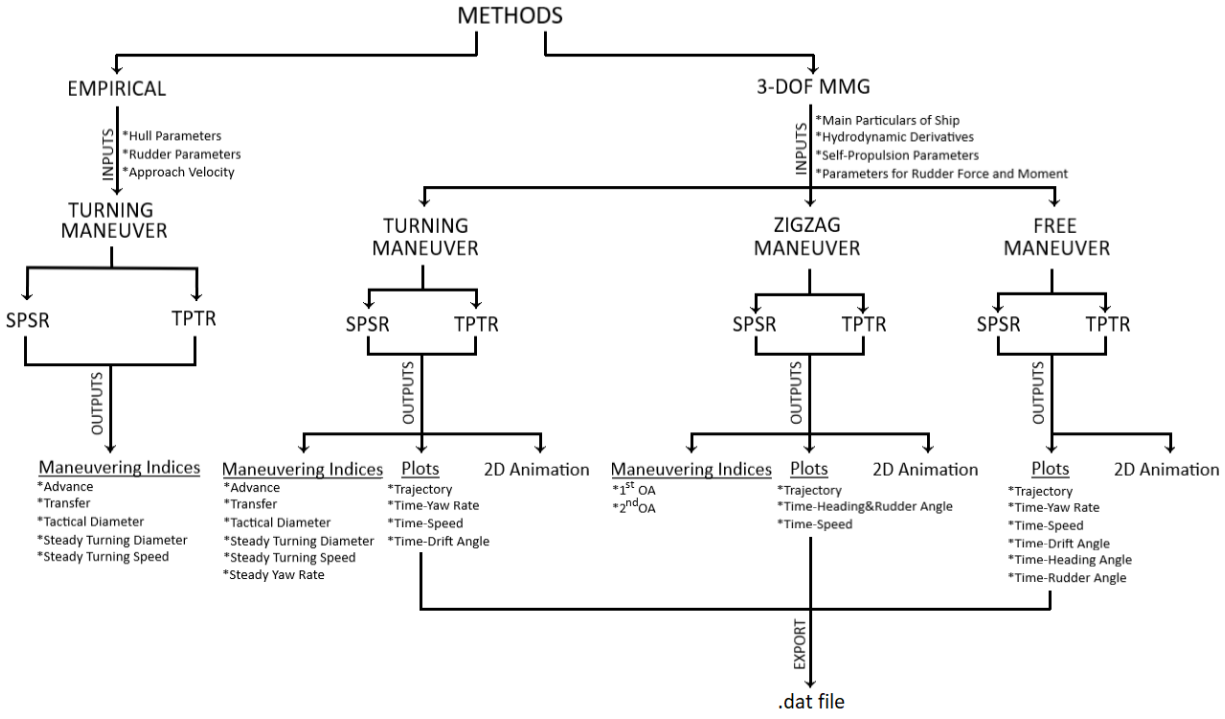

Figure 2. Workflow scheme of MANSIM.

Main solver code and functions of MANSIM were developed in MATLAB environment. GUI was created with MATLAB Guide Layout editor which allows user to design different kinds of user interfaces with some basic tools (menus, toolbars, buttons, sliders, etc.). In the input section of MANSIM, parameters required for mathematical model can be imported from a premade ".txt" file using the corresponding icon in toolbar instead of filling the text boxes one by one. Alternatively, if user has no input parameters except the main dimensions of ship, all inputs related to hull, propeller(s) and rudder(s) can be calculated automatically by MANSIM using available empirical formulas embedded in software.

Obtained outputs can be examined on user interface or can be exported as ".dat" file. It is also possible to visualize the trajectory of ships during turning/zigzag/free maneuvers as 2D animation. Sample screenshots of input and output sections of MANSIM are shown in Figures 3-4. Pop-ups near some parameters in the input screen are used for selecting empirical formulas embedded in the code. Note that the parameters of propeller and rudder in TPTR option have double values different from SPSR configuration, since TPTR ships may have different values for each parameter of rudder and propeller.

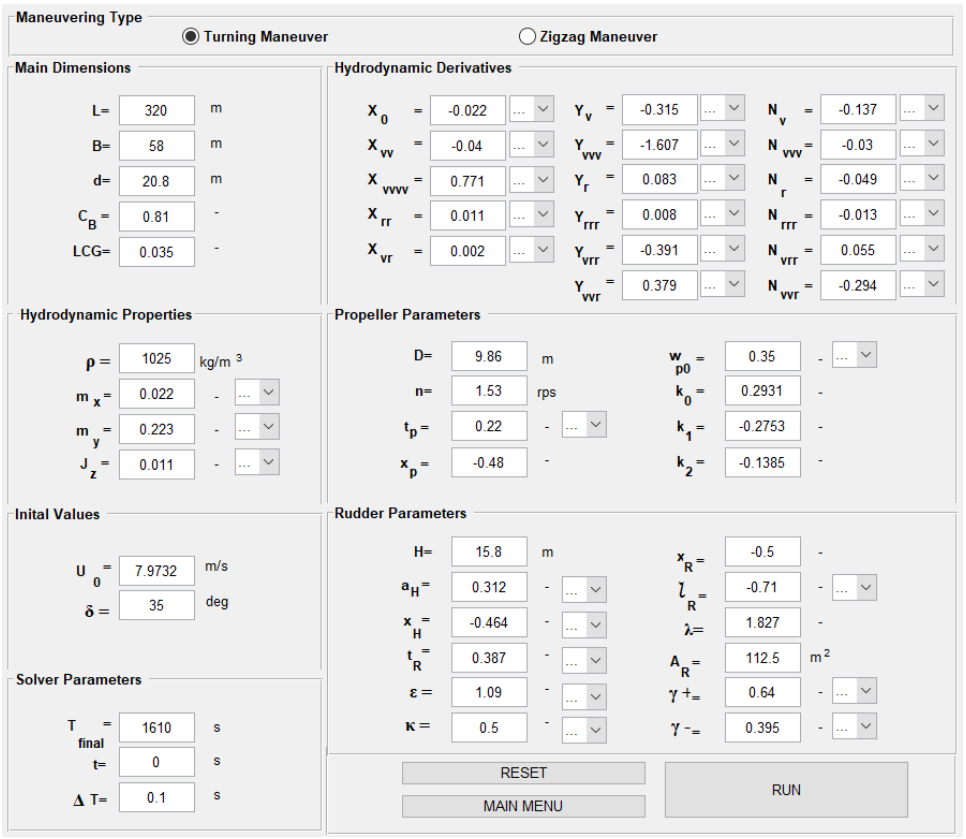

Figure 3. Sample screenshot of input section of 3DOF-MMG approach in MANSIM.

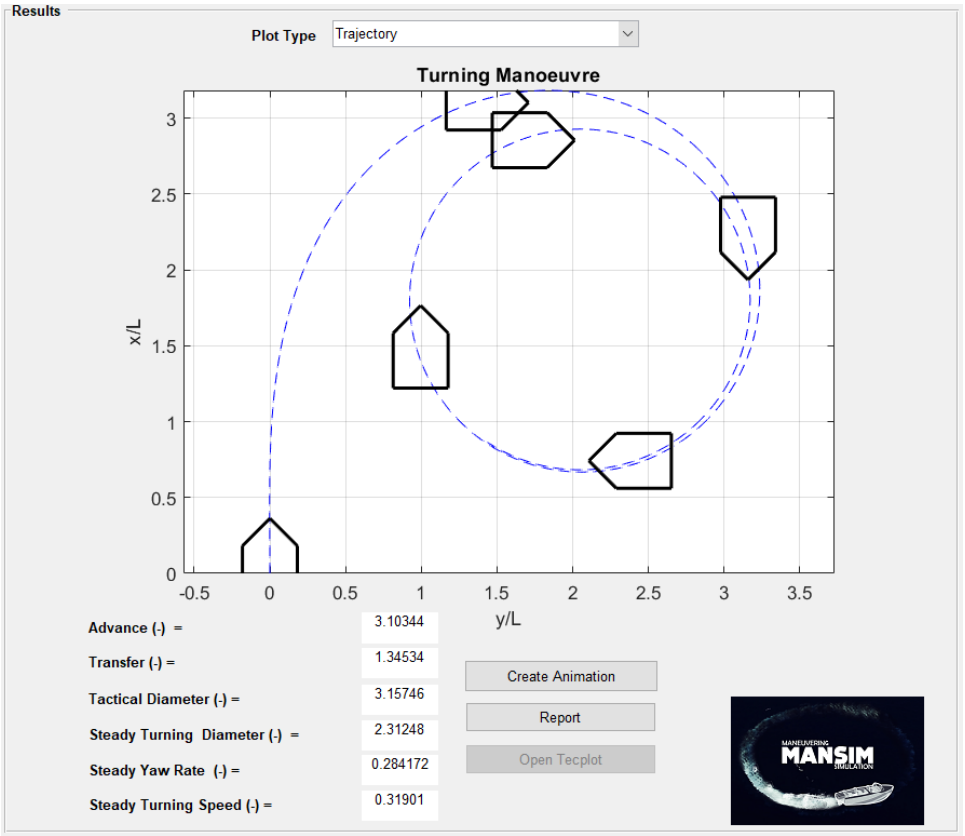

Figure 4. Sample screenshot of output section of turning/zigzag maneuver in MANSIM.

5 Application of MANSIM to Benchmark Ships

In this section, turning and zigzag maneuvers computed by MANSIM were validated for two benchmark ships, namely, KVLCC2 and DTMB5415 hulls. KVLCC2 tanker is a SPSR ship, while DTMB5415 has a TPTR configuration. Mathematical models for these type of ships are available in MANSIM and these models are described in section 2.2. Available experimental and computational results for hydrodynamic derivatives, rudder force and self-propulsion parameters were used to compare the turning and zigzag maneuvers for both ships. Numerically obtained hydrodynamic derivatives have free surface effects taken into account since both ships have relatively high Froude numbers (Kinaci et al., 2016). Simulation results were compared with free running data available in literature. Furthermore, influence of variation of hydrodynamic derivatives and rudder parameters on maneuvering indices such as advance, tactical diameter, overshoot angles, etc. were investigated systematically by performing a comprehensive sensitivity analysis.

5.1 Simulation of Turning and Zigzag Maneuvers of KVLCC2

Turning and zigzag maneuvers of full-scale KVLCC2 tanker have been simulated by MANSIM by using hydrodynamic derivatives, rudder and propeller parameters given in Yasukawa and Yoshimura (2015) who have conducted circular motion and rudder force tests for the 1/110 scaled model of KVLCC2. Free running results are also available for this ship and these tests have been carried out by MARIN for the 1/45.7 scaled model (ftp://ftp.forcetechnology.com). Maneuvering results of $35°$ and $-35°$ turning circle, and $10/10$, $-10/-10$, $20/20$, $-20/-20$ zigzag maneuvers predicted by MANSIM were compared with results of free running tests for full-scale KVLCC2. Input parameters of MANSIM for the prediction of maneuvering performance are given in Table 18. Comparison of results for port and starboard turnings are shown in Figures 5 and 6. Note that both results are in good agreement.

Table 18. Inputs of MANSIM for prediction of maneuvering abilities of full-scale KVLCC2.

Main Particulars							
$L_{pp}(m)$	320	$B(m)$	58	$d(m)$	20.8	C_B	0.81
$GM(m)$	5.71	$x_G(m)$	11.1	$\nabla(m^3)$	312622	Fr	0.142
Hydrodynamic Derivatives							
X'_0	0.022	m'_x	0.022	Y'_{vrr}	-0.391	N'_r	-0.049
X'_{vv}	-0.040	Y'_v	-0.315	Y'_{vvr}	0.379	N'_{rrr}	-0.013
X'_{vvvv}	0.771	Y'_{vvv}	-1.607	m'_y	0.223	N'_{vrr}	0.055
X'_{rr}	0.011	Y'_r	0.083	N'_v	-0.137	N'_{vvr}	-0.294
X'_{vr}	0.002	Y'_{rrr}	0.008	N'_{vvv}	-0.030	J'_z	0.011
Components of Propeller Force							
$D_P(m)$	9.86	t_P	0.22	k_1	-0.275	k_0	0.293
$n_P(rps)$	1.53	w_{P0}	0.35	k_2	-0.139	x_P	-0.48
Components of Rudder Forces and Moment							
$H_R(m)$	15.8	λ	1.827	x'_H	-0.464	l'_R	-0.71
x'_R	-0.50	a_H	0.312	ε	1.09	$\gamma_R\ (\beta_R < 0)$	0.395
$A_R(m^2)$	112.5	t_R	0.387	κ	0.50	$\gamma_R\ (\beta_R > 0)$	0.64

Turning maneuver indices such as advance (Ad), transfer (Tr), tactical diameter (TD), steady turning diameter (STD), steady yaw rate (SYR), steady turning speed (STS) and steady drift angle (SDA) were obtained for the full-scale KVLCC2 tanker and shown in Table 19. It can be said that the results calculated by MANSIM agree well with the free running data. History of kinematical parameters was underpredicted slightly except steady yaw rate that has a perfect match. Largest difference is around 20% in speed reduction. However, this discrepancy can also be attributed to the differences in propeller rotation rate. Calculations are based on the self-propulsion point of the full-scale ship whereas the free running tests are conducted by self-propulsion point of model ship. This is most likely the primary reason of differences in the turning circle trajectories. It can also be stated that the results of empirical approach seem to be in accordance with experiments.

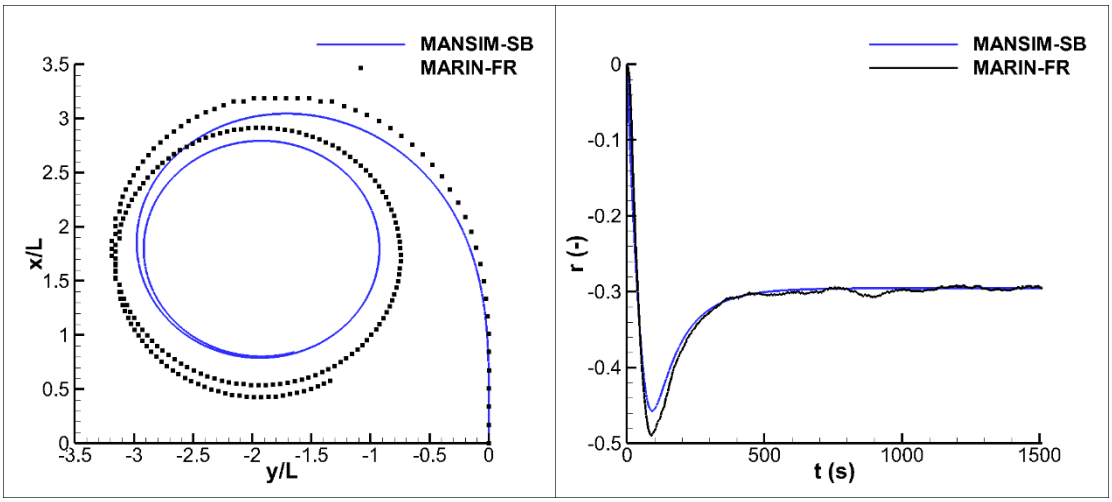

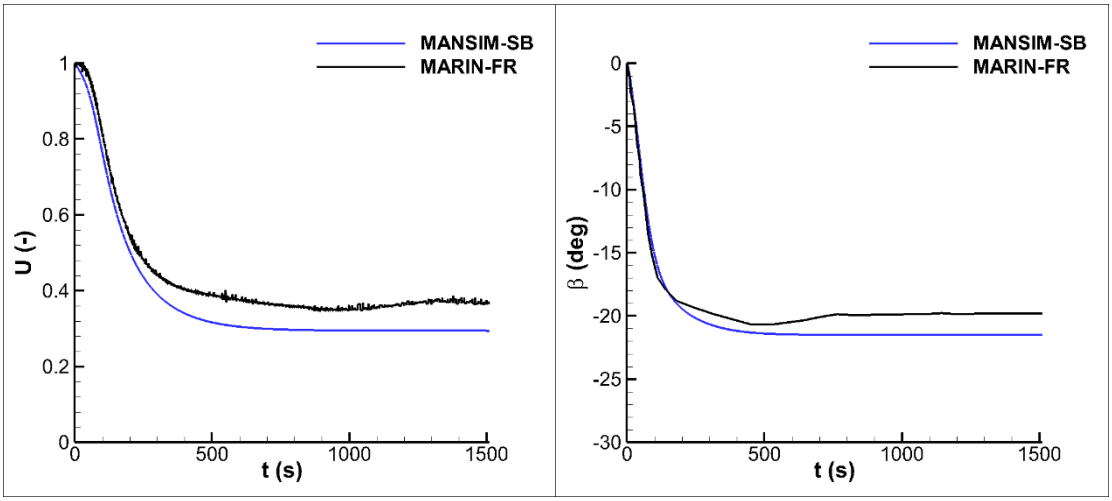

Figure 5. Comparison of $-35°$ turning maneuver results of KVLCC2 by MANSIM with free running (FR) data ($Fr = 0.142$).

Table 19. Comparison of turning maneuver indices of full-scale KVLCC2.

	$\delta = -35°$				$\delta = 35°$			
Maneuvering Indices	MARIN FR	MANSIM SB	Yasukawa SB (2015)	Lyster EMP (1979)	MARIN FR	MANSIM SB	Yasukawa SB (2015)	Lyster EMP (1979)
Ad (-)	3.11	3.10	3.56	2.76	3.25	3.10	3.67	2.76
Tr (-)	-1.22	-1.23	-1.51	-1.30	1.36	1.35	1.58	1.30
TD (-)	-3.08	-2.90	-3.59	-2.75	3.34	3.16	3.71	2.75
STD (-)	2.48	2.05	-	2.06	2.54	2.31	-	2.06
SYR (-)	-0.30	-0.30	-	-	0.29	0.28	-	-
STS (-)	0.36	0.29	-	0.35	0.38	0.32	-	0.35
SDA (deg)	-19.83	-21.51	-	-	18.59	20.24	-	-

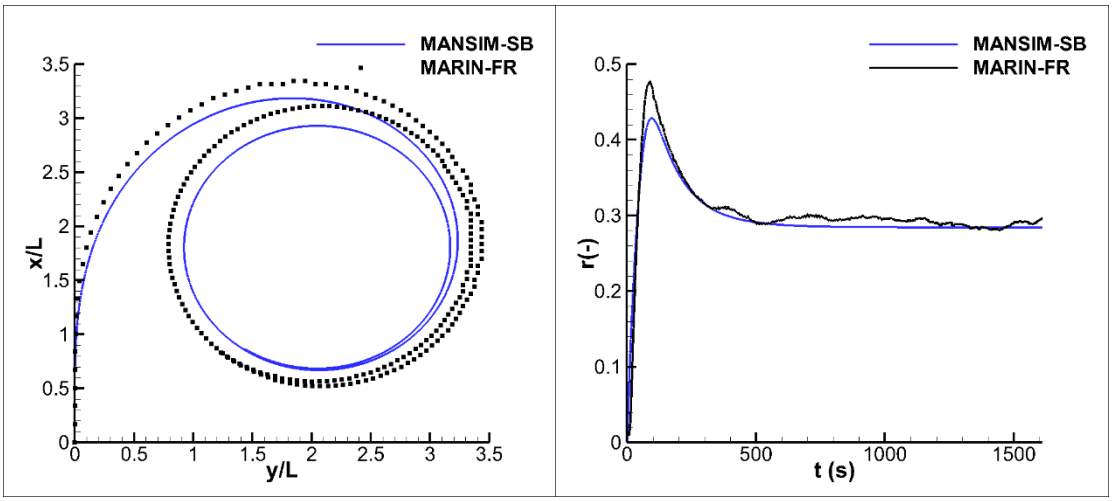

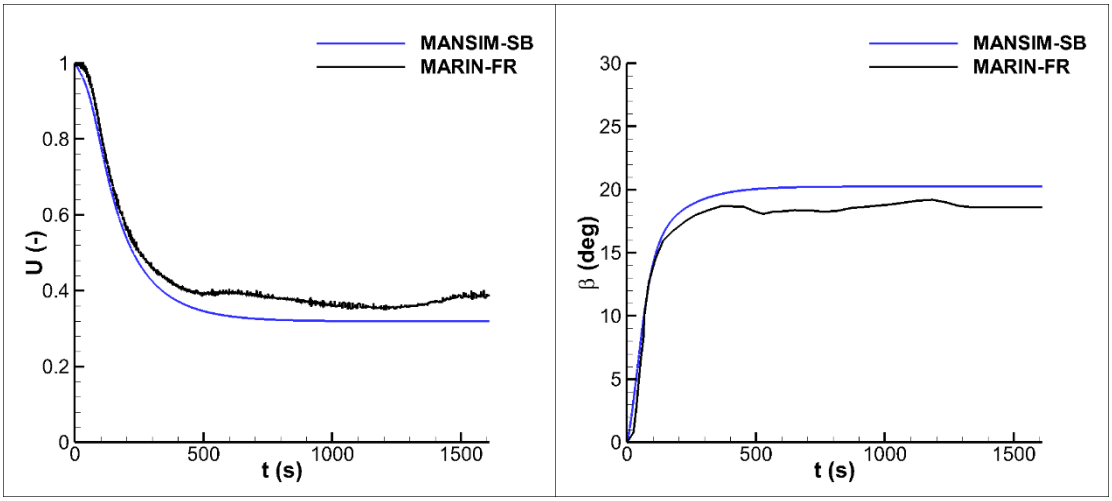

Figure 6. Comparison of $35°$ turning maneuver results of KVLCC2 by MANSIM with free running (FR) data ($Fr = 0.142$).

Comparison of various type of predicted zigzag maneuvers with free running data for full-scale KVLCC2 is shown in Figures 7-10. Agreement in the first overshoot angles (OA) are better than the second overshoot angles for both $-10/-10$ and $10/10$ zigzag maneuvers. OAs in $-20/-20$ and $20/20$ zigzag maneuvers are shown in Figures 9-10 and general trend of zigzag motion agree well with the free running data. It can also be deduced from these figures that the phase shifts in trajectories are generally caused by the mismatch in rudder execution times.

Maneuvering indices of zigzag motion are considered as 1^{st} and 2^{nd} OAs for $-10/-10$, $10/10$, $-20/-20$ and $20/20$ maneuvers, and comparison of results are given in Table 20. Scale effect could be a reason for these discrepancies since the hydrodynamic derivatives and other parameters have been obtained at model scale of ship. Furthermore, a more precise prediction method may be required to improve the accuracy of results instead of using empirical approaches for the terms of added mass and added moment of inertia. It should also be noted that the accuracy of prediction was found to be strongly related with the initial conditions (approach speed, rudder angle, propeller rate, etc.) in zigzag maneuvers.

Table 20. Comparison of predicted maneuvering indices of full-scale KVLCC2 with free running data in zigzag motions.

Maneuver	OAs (deg)	MARIN-FR	MANSIM-SB	Yasukawa-SB (2015)
$-10/-10$	1^{st}	9.5	7.5	8.8
	2^{nd}	15	9.4	12.6
$10/10$	1^{st}	8.2	5.3	5.8
	2^{nd}	21.9	14.1	20.5
$-20/-20$	1^{st}	15.1	14.2	16.1
	2^{nd}	13.3	11.8	14.6
$20/20$	1^{st}	13.7	11.1	11.8
	2^{nd}	14.9	15.5	19.7

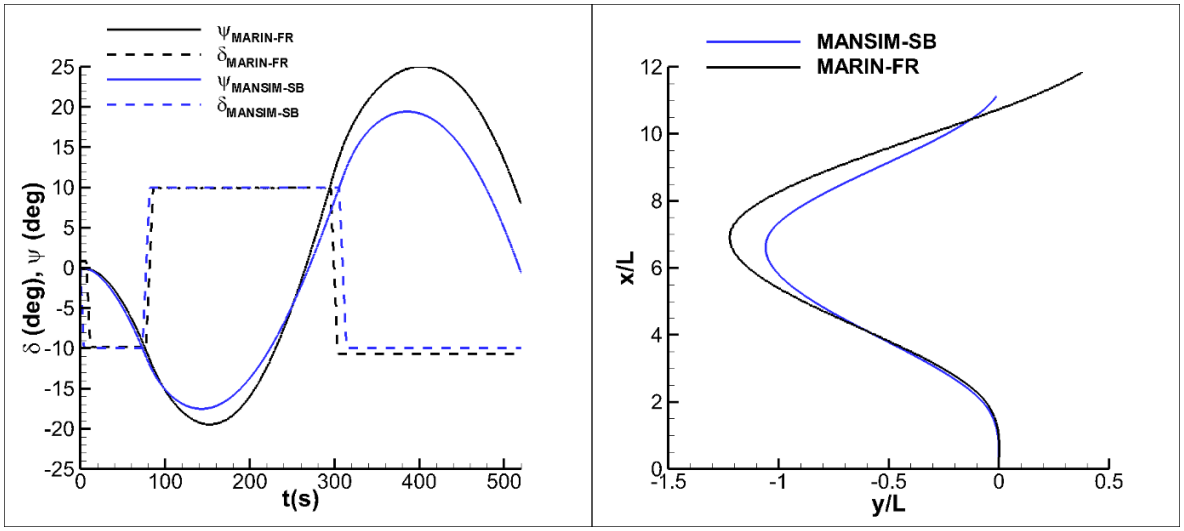

Figure 7. Comparison of predicted heading angle, rudder angle and trajectory with free running (FR) data in $-10/-10$ zigzag maneuver ($Fr = 0.142$).

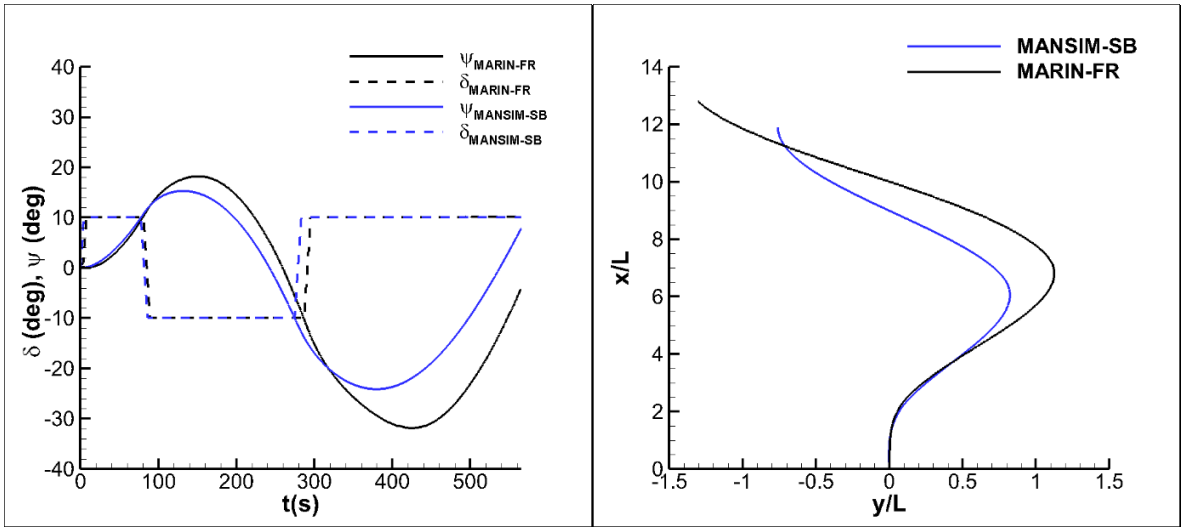

Figure 8. Comparison of predicted heading angle, rudder angle and trajectory with free running (FR) data in $10/10$ zigzag maneuver ($Fr = 0.142$).

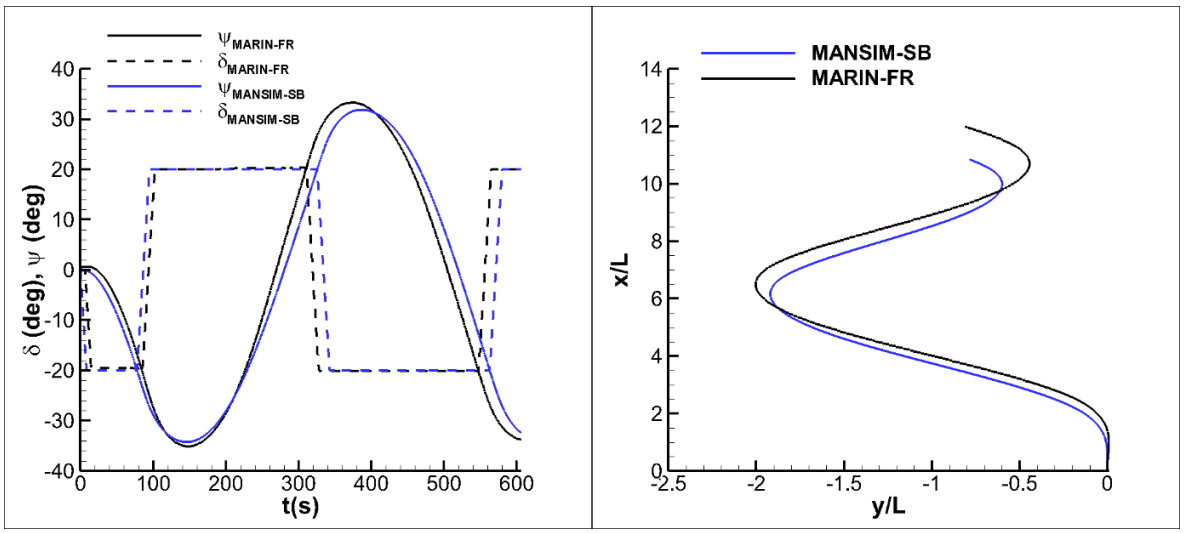

Figure 9. Comparison of predicted heading angle, rudder angle and trajectory with free running (FR) data in $-20/-20$ zigzag maneuver ($Fr = 0.142$).

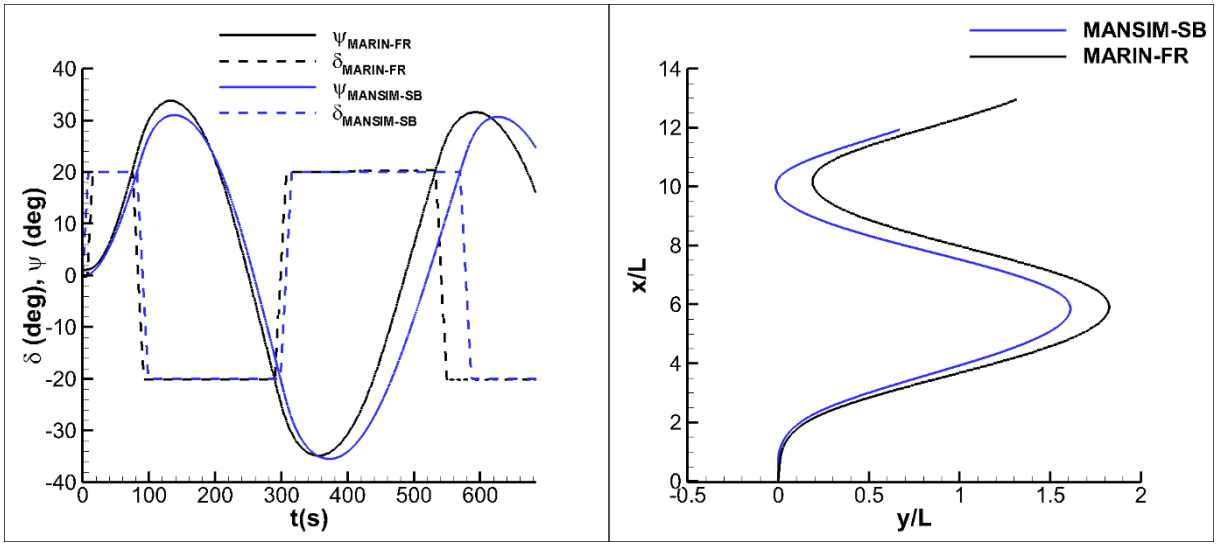

Figure 10. Comparison of predicted heading angle, rudder angle and trajectory with free running (FR) data in $20/20$ zigzag maneuver ($Fr = 0.142$).

5.2 Simulation of Turning and Zigzag Maneuvers of DTMB5415

After performing a maneuvering simulation for KVLCC2, a system-based simulation was also carried out for full-scale DTMB5415 surface combatant by using MANSIM to predict its turning and zigzag maneuverabilities. Hydrodynamic derivatives and other parameters related to the propeller and rudder were computed by CFD for the 1/46.588 scaled model of DTMB5415 hull (Sukas et al., 2019). Since DTMB5415 has a TPTR configuration, propeller and rudder parameters may show difference due to asymmetric flow around the control surfaces during maneuvering motion. For validation, system based (SB) simulation results of 35 and -35 turning maneuvers, and -20/20 zigzag manuever were compared with those of free running tests carried out by MARIN (ftp://ftp.forcetechnology.com). Input parameters of MANSIM for full-scale DTMB5415 hull are given in Table 21. Parameters with superscripts "S" and "P" indicate the values for starboard and port sides, respectively. Predicted results of trajectory, yaw rate and speed loss were compared with experimental data for -35 and 35 turning maneuvers and shown in Figures 11-12.

Table 21. Inputs of MANSIM for prediction of maneuvering abilities of full-scale DTMB5415.

Main Particulars							
$L_{pp}(m)$	142	$B(m)$	19.06	$d(m)$	6.15	C_B	0.507
$GM(m)$	1.95	$x_G(m)$	-0.652	$\nabla(m^3)$	8424.4	Fr	0.248
Hydrodynamic Derivatives							
X'_0	0.016	Y'_v	-0.294	Y'_{vvr}	-1.506	N'_{rrr}	-0.048
X'_{vv}	-0.182	Y'_{vvv}	-1.174	m'_y	0.108	N'_{vrr}	-0.218
X'_{rr}	-0.028	Y'_r	-0.047	N'_v	-0.162	N'_{vvr}	-0.800
X'_{vr}	-0.093	Y'_{rrr}	-0.052	N'_{vvv}	-0.225	J'_z	0.008
m'_x	0.007	Y'_{vrr}	-0.784	N'_r	-0.045		
Components of Propeller Force and Moment							
$D_P^{P,S}(m)$	6.15	$t_P^{P,S}$	0.210	$k_0^{P,S}$	0.398	$k_1^{P,S}$	-0.299
$n_P^{P,S}(rps)$	1.65	$w_{P0}^{P,S}$	0.073	$k_2^{P,S}$	-0.141	$x_P'^{P,S}$, $\lvert y_P'^{P,S}\rvert$	-0.462, 0.244
Components of Rudders Force and Moment							

$H_R^{P,S}(m)$	4.38	$a_H^{P,S}$	0.086	$\varepsilon^{P,S}$	0.93;1.00	$x_R'^{P,S}, \lvert y_R'^{P,S} \rvert$	-0.472, 0.267
$\lambda^{P,S}$	1.26	$t_R^{P,S}$	0.440	$\kappa^{P,S}$	0.62;0.70	$\gamma_R^{P,S}\ (\beta_R < 0)$	0.53;0.37
$A_R^{P,S}(m^2)$	15.4	$x_H'^{P,S}$	-0.437	$l_R'^{P,S}$	-0.944	$\gamma_R^{P,S}\ (\beta_R > 0)$	0.37;0.53

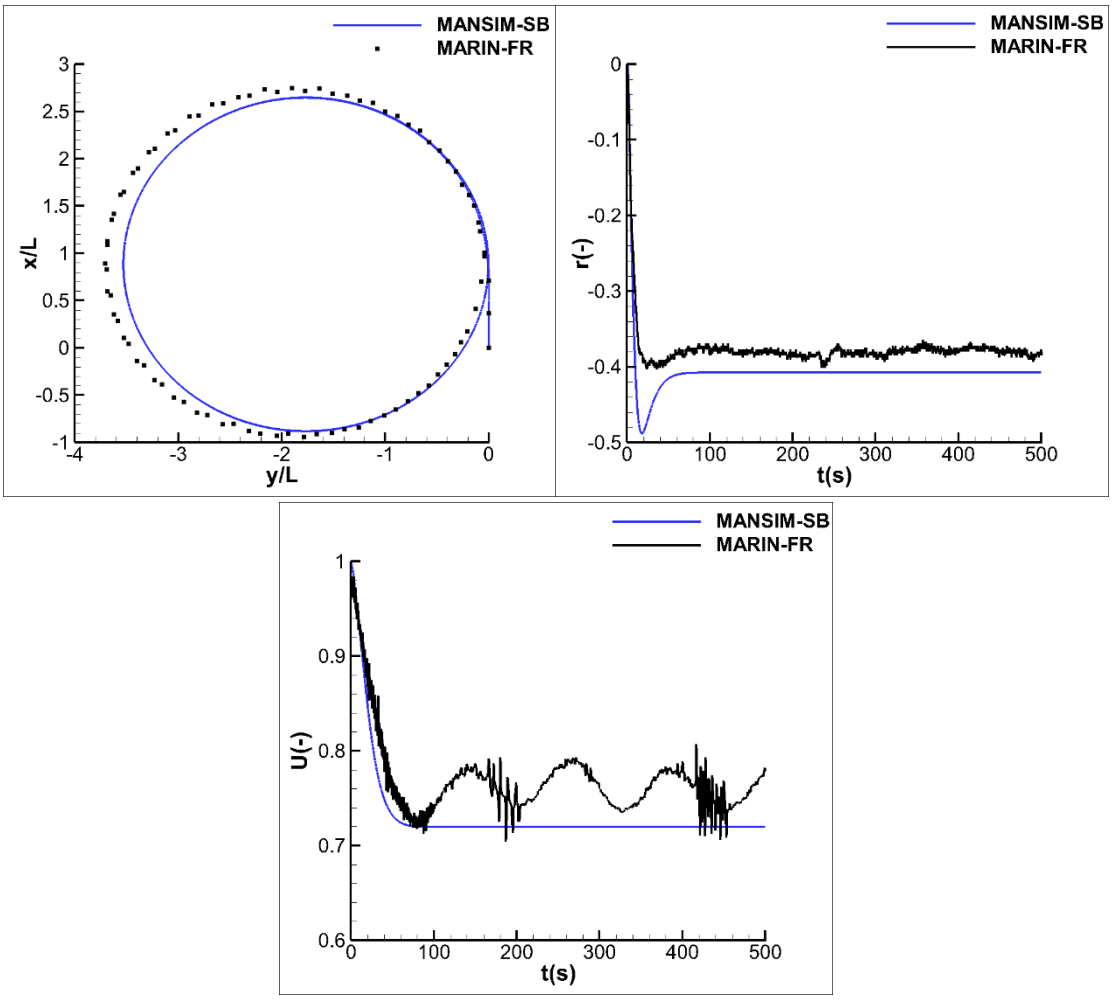

Figure 11. Comparison of $-35°$ turning maneuver results of DTMB5415 by MANSIM with free running (FR) data ($Fr = 0.25$).

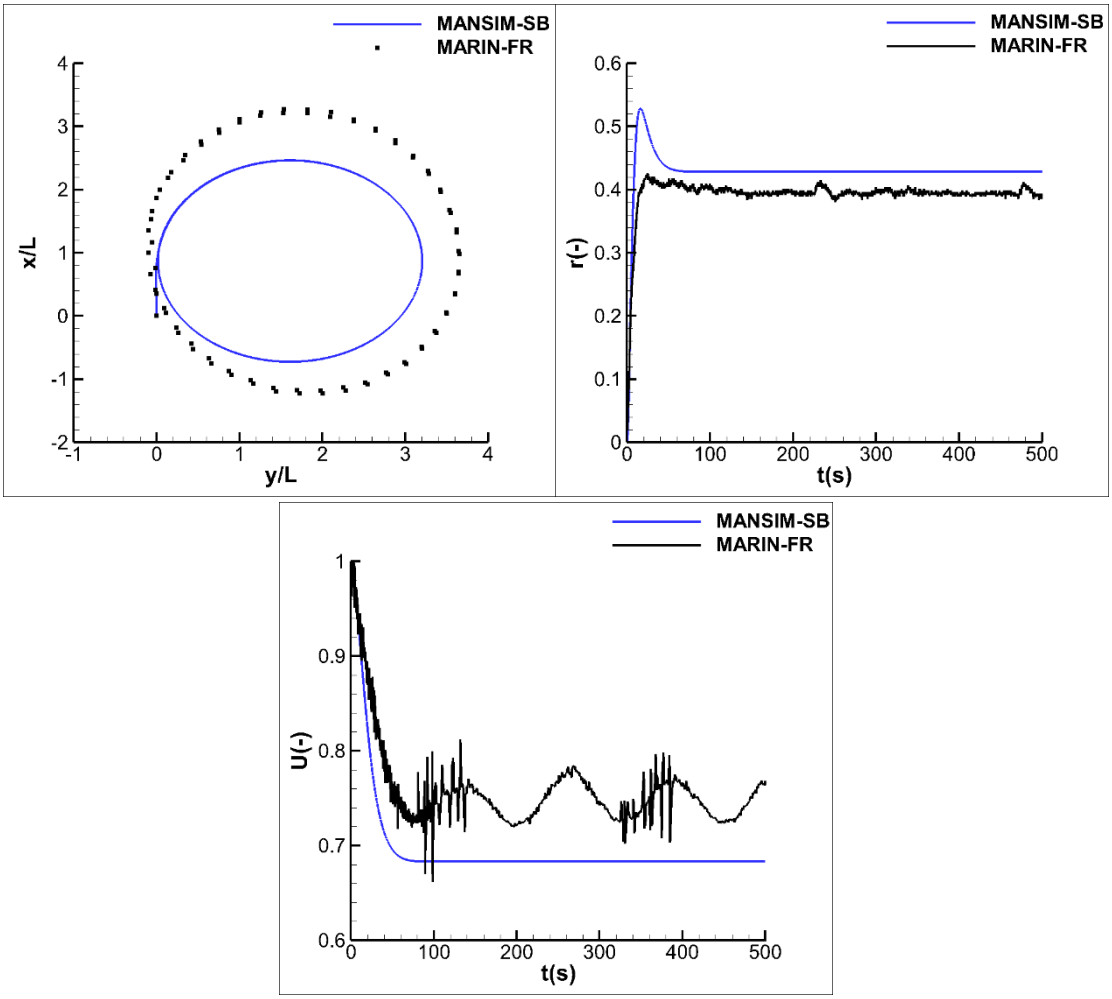

Figure 12. Comparison of $35°$ turning maneuver results of DTMB5415 by MANSIM with free running (FR) data ($Fr = 0.25$).

According to the results shown in Figures 12-13, free running data seems to have larger difference in port and starboard turnings than those of MANSIM. This discrepancy in experiments can be due to asymmetry between the values of rudder parameters for port and starboard turnings. On the other hand, there is a large relative difference between MANSIM and free running data in starboard turning for DTMB5415 hull. Such difference is most likely due to symmetry assumption for the rudder and propeller parameters in CFD analyses. Because all necessary rudder and propeller parameters of DTMB5415 hull were estimated by CFD analyses [3] for port turning. Additionally, it was assumed that these parameters are identical/symmetrical with the starboard turning. Another possible reason for the discrepancies in Figures 12-13 may be caused by neglecting the roll-coupled effects for DTMB5415 hull. Yaw rate of ship was slightly overestimated by MANSIM which leads to a smaller turning trajectory prediction. Speed reduction percentages during maneuver were estimated higher than the free running results for both side turnings. Turning maneuver indices of full-scale DTMB5415 are given in Table 22. The results obtained by empirical approach also seem to be underpredicted as compared to the experiments.

Table 22. Comparison of turning maneuver indices of full-scale DTMB5415.

Maneuvering Indices	$\delta = -35°$				$\delta = 35°$			
	MARIN FR	MANSIM SB	Carrica CFDB (2013)	Lyster EMP (1979)	MARIN FR	MANSIM SB	Carrica CFDB (2013)	Lyster EMP (1979)
Ad (-)	2.71	2.59	2.90	2.55	3.19	2.40	2.90	2.55
Tr (-)	-1.46	-1.35	-1.58	-1.15	1.33	1.17	1.58	1.15
TD (-)	-3.65	-3.48	-3.87	-2.83	3.60	3.14	3.87	2.83
STD (-)	3.66	3.53	-	2.69	3.75	3.19	-	2.69
SYR (-)	-0.38	-0.41	-	-	0.39	0.43	-	-
STS (-)	0.75	0.72	-	0.62	0.74	0.68	-	0.62

Predicted heading/rudder angles and trajectory for $-20/-20$ zigzag maneuver were also compared with free running data and shown in Figure 13. Despite a good agreement of the predicted overshoot angles with the experiments, there is a discrepancy in trajectories due to the early execution time of second and third deflections of rudder in the system-based simulation. Maneuvering indices of zigzag motion were compared in terms of 1^{st} and 2^{nd} OAs and given in Table 23. As mentioned previously, accuracy of results can be influenced by slight differences with the experimental procedure such as initial conditions of the model. It can also be noted that the results by MANSIM are based on self-propulsion point of the full-scale ship whereas free running tests are conducted by self-propulsion point of the model ship. This can be another reason for the differences in the turning and zigzag trajectories of DTMB5415 hull.

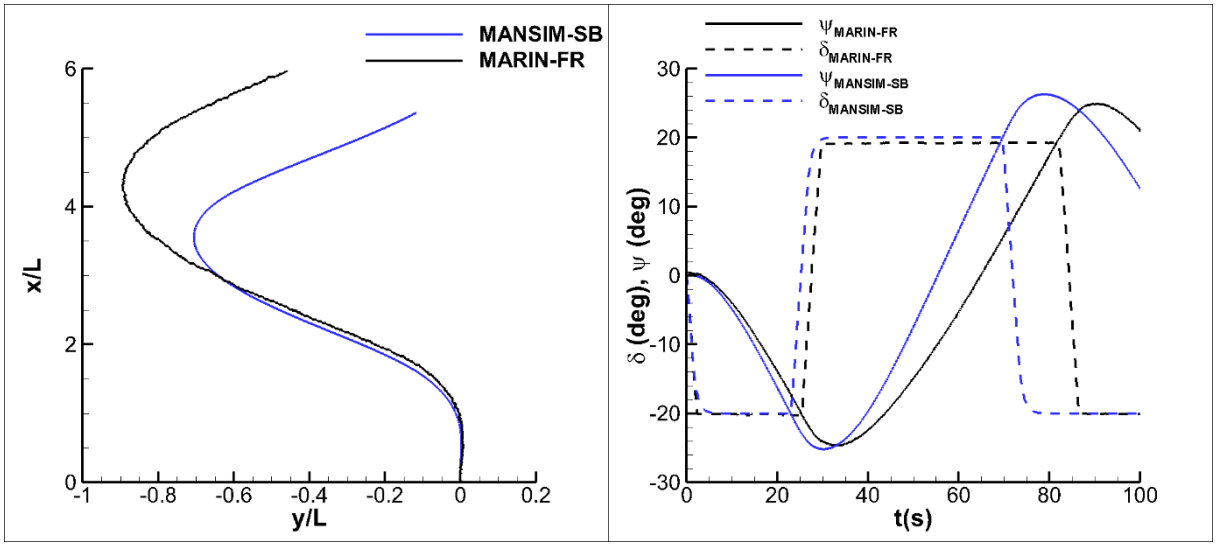

Figure 13. Comparison of predicted heading angle, rudder angle and trajectory of full-scale DTMB5415 with free running (FR) data in $-20/-20$ zigzag maneuver ($Fr = 0.25$).

Table 23. Comparison of predicted maneuvering indices of full-scale DTMB5415 with free running data in $-20/-20$ zigzag maneuver.

Maneuver	OAs (deg)	MARIN-FR	MANSIM-SB	Carrica-CFDB
$-20/-20$	1^{st}	4.70	5.12	7.30
	2^{nd}	4.80	6.34	7.20

5.3 Sensitivity Analysis of Hydrodynamic Derivatives and Rudder Parameters

Standard MMG model used in MANSIM consists total of 17 hydrodynamic derivatives in the maneuvering equations of motion. In addition, propeller and rudder parameters are included into these equations to simulate free running tests. Utilizing the user interface of MANSIM, parametrical studies such as sensitivity analysis can be performed readily. Effect of any parameter on general maneuvering performance of ships can be investigated in detail. Here, a sensitivity analysis was performed for KVLCC2 and DTMB5415 ships to investigate the effect of each hydrodynamic derivative and rudder parameters on the turning and zigzag maneuverabilities. $-35°$ turning and $-20°/-20°$ zigzag maneuvers were selected as sample cases to be examined. Influence of variation of hydrodynamic derivatives/rudder parameters on maneuvering indices such as advance (Ad), transfer (Tr), tactical diameter (TD), steady turning diameter (STD) and overshoot angles (OA) were investigated. Original value of parameters was increased seperately by 25% and these values were used in the mathematical model. Sensitivity analysis was carried out by using the index proposed by Sen (2000). This analysis was adopted to examine the variation of maneuvering indices caused by changes in each hydrodynamic derivative and rudder parameter. Sensitivity index S is represented as given in Eqn. 21:

$$S = \frac{(R - R^*)/R^*}{(H - H^*)/H^*} \tag{21}$$

where, R^* and H^* denote the original values of maneuvering index and corresponding hydrodynamic derivative/rudder parameter, respectively. R and H represent increased values by 25%. After calculating S, all these values of parameters are summed up and a total value for each indice is obtained. Then, sensitivity index for each parameter is divided by the total value of this indice. For example, percentage of the effect of X_0' in advance is calculated by,

$$\%S_{X_0',Ad} = 100 \cdot \frac{S_{X_0'}}{S_{Ad}} \tag{22}$$

Here; $\%S_{X_0',Ad}$ denotes the effect of X_0' in percentages, $S_{X_0'}$ is the sensitivity index of X_0' and S_{Ad} is the total sensitivity index value for advance index. Sensitivity of each parameter as a percentage for each maneuvering index for KVLCC2 and DTMB5415 are given in Tables 24 and 25. In these tables, parameters which have greater value than or at least equal to 10% were considered to be highly effective as shown in bold form. Parameters, which are between 3-10%, were considered to have mediocre at best as shown in underlined form.

Table 24. Sensitivity analysis of hydrodynamic derivatives and rudder parameters of KVLCC2 in turning and zigzag maneuvers.

Parameters	Turning Maneuver Indices				Zigzag Maneuver Indices	
	Ad	Tr	TD	STD	$1^{st}\ OA$	$2^{nd}\ OA$
X_0'	2.74	2.94	<u>3.17</u>	1.68	0.88	<u>3.99</u>
X_{vv}'	0.46	0.00	0.32	0.42	0.35	0.20
X_{vvvv}'	0.46	0.00	0.32	0.84	0.35	0.40
X_{rr}'	0.46	0.00	0.32	0.84	0.35	0.40
X_{vr}'	0.46	0.00	0.00	0.00	0.35	0.20
Y_v'	0.00	<u>5.88</u>	2.54	0.84	<u>8.13</u>	<u>5.59</u>
Y_{vvv}'	0.46	0.88	0.00	0.42	0.18	1.00
Y_r'	0.46	<u>3.82</u>	2.22	0.42	<u>5.30</u>	2.59
Y_{rrr}'	0.46	0.00	0.00	0.00	0.35	0.20
Y_{vrr}'	0.46	2.06	0.32	0.42	0.53	0.80

Y'_{vvr}	0.46	0.88	0.00	0.00	0.18	0.40
N'_v	**14.16**	**13.53**	**13.02**	6.95	**34.45**	**29.14**
N'_{vvv}	0.46	0.00	0.32	0.00	0.53	0.40
N'_r	**15.53**	**12.35**	**12.38**	8.21	**15.02**	**13.97**
N'_{rrr}	0.46	0.88	1.27	2.11	0.00	0.40
N'_{vrr}	1.37	2.06	2.54	2.95	0.18	1.00
N'_{vvr}	2.74	4.71	6.98	6.53	1.41	3.59
m'_x	0.46	0.88	0.00	0.42	2.30	1.20
m'_y	0.46	0.00	2.22	4.84	1.94	0.20
J'_z	1.83	0.00	0.32	0.00	3.36	4.39
a_H	4.11	2.94	2.54	2.53	1.41	2.79
x'_H	3.65	2.06	2.22	2.53	1.77	2.40
t_R	0.00	0.88	0.95	2.11	0.53	0.80
ε	**31.96**	**26.76**	**27.30**	**28.00**	6.01	**10.18**
κ	**11.42**	9.71	**11.75**	**19.79**	3.71	6.59
γ_R	2.74	3.82	4.44	4.21	6.71	0.80
l'_R	1.83	2.94	2.54	2.95	3.71	6.39

According to Table 24, hydrodynamic derivatives related to surge force X have lower effect on the obtained results than that of sway force and yaw moment derivatives. Only resistance coefficient X'_0 has a moderate effect on transfer, tactical diameter and second overshoot angles. First order derivatives seem to have a strong influence on maneuvers especially on zigzag indices, where N'_v has the highest impact among all. High order and coupled derivatives have lower effect on maneuvering indices except N'_{vvr}. Terms of added mass and added moment of inertia have a moderate effect on first overshoot angle, while only m'_y has a moderate effect on steady turning radius. Rudder parameters have also major influence on maneuvering indices. Particularly, variation of ε and κ greatly affects the turning and zigzag maneuvers of ship. It can briefly be stated for sensitivity analysis of KVLCC2 tanker that the overshoot angles are more sensitive to the variations of hydrodynamic derivatives and rudder parameters than those of turning maneuver. In addition, advance distance and steady turning diameter seem to be the least and most influenced indices by the variation of parameters in turning maneuver, respectively.

Table 25. Sensitivity analysis of hydrodynamic derivatives and rudder parameters of DTMB5415 in turning and zigzag maneuvers.

Parameters	Turning Maneuver Indices				Zigzag Maneuver Indices	
	Ad	Tr	TD	STD	$1^{st}\ OA$	$2^{nd}\ OA$
X'_0	0.82	0.00	0.00	0.00	2.15	2.85
X'_{vv}	0.00	0.00	0.00	0.00	0.66	0.67
X'_{rr}	0.00	0.00	0.00	0.00	0.83	0.67
X'_{vr}	0.00	0.00	0.00	0.00	0.83	1.34
Y'_v	2.45	4.16	0.00	0.71	2.48	1.68
Y'_{vvv}	0.82	0.83	0.00	0.36	0.33	0.84
Y'_r	0.82	1.66	0.35	0.36	1.49	0.50
Y'_{rrr}	0.00	0.00	0.00	0.00	0.33	0.50
Y'_{vrr}	2.45	2.49	0.35	0.71	0.66	0.50
Y'_{vvr}	3.27	1.66	1.75	1.79	1.49	0.67
N'_v	**13.88**	**10.80**	**14.39**	**14.29**	**17.36**	**15.10**
N'_{vvv}	1.22	0.83	1.05	1.07	0.83	0.17
N'_r	**11.84**	9.14	**10.88**	**11.07**	8.60	7.55
N'_{rrr}	3.27	3.32	3.51	3.57	0.50	2.01
N'_{vrr}	6.94	5.82	7.72	7.14	2.98	3.52

N'_{vvr}	9.39	9.97	**12.63**	**12.14**	3.31	4.70
m'_x	0.00	0.00	0.00	0.00	0.83	0.67
m'_y	0.00	0.83	0.35	0.00	1.49	0.67
J'_z	1.22	0.00	0.00	0.00	4.13	3.02
a_H	0.82	0.00	0.35	0.00	0.00	1.17
x'_H	0.00	0.83	0.35	0.36	0.33	0.50
t_R	3.27	2.49	3.16	3.21	0.17	0.50
ε	**10.20**	0.00	2.46	2.50	**16.03**	**18.29**
κ	0.82	0.83	0.00	0.36	3.14	6.21
γ_R	**15.92**	**26.32**	**24.21**	**23.93**	**17.02**	**15.27**
l'_R	**10.61**	**18.01**	**16.49**	**16.43**	**12.07**	**10.40**

Table 25 shows the sensitivity indices of turning and zigzag maneuver of DTMB5415 hull. Note that the parameters of port and starboard rudders of DTMB5415 are increased together. Similar to KVLCC2 hull, N'_v was found to be the most dominant linear derivative in both turning and zigzag maneuvers of DTMB5415 hull. Nonlinear derivatives have small effects except N'_{rrr} which affects the manuevers moderately. Coupled derivatives related to the yaw moment (N'_{vvr}, N'_{vrr}) have relatively major impact as compared to those of surge and sway forces. X'_{vv}, X'_{rr}, X'_{vr}, Y'_{rrr} and m'_x have almost no influence on the indices of turning maneuver. Rudder parameters have a significant effect on the maneuvers rather than the hydrodynamic derivatives. Additionally, similar to KVLCC2 case, advance distance was found to be the least influenced index from the variation of hydrodynamic derivatives and rudder parameters. On the whole, it can be noted for both ships that the derivatives based on yaw moment are highly influential on turning and zigzag maneuvers. Indices of zigzag motion are oversensitive to the variation of parameters in MMG model. Terms of added mass and added moment of inertia have relatively low effect than the other parameters especially in turning motion. Thus, they are generally estimated based on empirical formulas or charts. Results of sensitivity analysis for both ships are summarized in Table 26.

Table 26. Parameters that have high or mediocre impact for turning circle and zigzag maneuvers.

	Turning Maneuver				**Zigzag Maneuver**			
	KVLCC2		DTMB5415		KVLCC2		DTMB5415	
Impact Level	High	Mediocre	High	Mediocre	High	Mediocre	High	Mediocre
Hydrodynamic derivatives	N'_v, N'_r	N'_{vvr}	N'_v, N'_r, N'_{vvr}	$Y'_v, Y'_{vvr}, N'_{rrr}, N'_{vrr}$	N'_v, N'_r	Y'_v, Y'_r, J'_z	N'_v	$N'_r, N'_{vvr}, N'_{vrr}, J'_z$
Rudder parameters	ε, κ	γ_R	$\varepsilon, \gamma_R, l'_R$	t_R	ε	κ, γ_R, l'_R	$\varepsilon, \gamma_R, l'_R$	κ

5.4 Effect of linear derivatives on maneuvering indices

In the previous section, sensitivity analyses showed the significance of each parameter on maneuvering indices. However, how these parameters change maneuvering indices are still unknown. This section is devoted to the effect of linear derivatives on maneuvering indices of KVLCC2 to reveal how they change turning and zigzag maneuvers. To do this, linear derivatives (Y_v, Y_r, N_v and N_r) were changed by a considerable amount and results were plotted. Only one derivative was changed at a time to particularly show corresponding effect. Some interesting observations were noted:

- There is an optimum value for Y_v to minimize advance and steady turning diameter.
- Y_r also has an optimum value for minimizing steady turning diameter.

- Decrease in the magnitude of N_v results in increase in some maneuvering indices such as advance, transfer, steady turning diameter and tactical diameter of turning circle test. On the other hand, it enhances zigzag test by decreasing 1st and 2nd overshoot angles.
- Decrease in the magnitude of N_r results in decrease in some maneuvering indices such as advance, transfer, steady turning diameter and tactical diameter of turning circle test. Nevertheless, overshoot angles in zigzag test considerably increase.

Observations from these graphs may be elaborated but points listed above have primary importance for turning and zigzag tests. Graphs for Y_v are given in Figure 14, Y_r in Figure 15, N_v in Figure 16 and N_r in Figure 17.

6 Conclusions

In this study, a user-friendly ship maneuvering code based on MMG mathematical model has been introduced. Graphical user interface of code allows to make an easy and simple changes to hydrodynamic derivatives or propeller/rudder parameters. This software provides a basis for researchers to experiment with all coefficients / parameters and to have a better understanding of ship maneuvering phenomena which involves a dynamic and complex background. It also contains many empirical relations suggested by many researchers in the field of ship maneuvering. MANSIM is considered to be helpful especially for sensitivity analysis on maneuvering. A SPSR and a TPTR ship have been investigated and parameters that have significant effect on each maneuvering indice have been found. Findings can be listed as follows:

- N_v and N_r are highly effective on maneuvering indices.
- ε is a highly effective rudder parameter in ship maneuvering.
- Coupled terms have a non-negligible importance for DTMB5415 ship.
- Rudder parameters have higher importance in zigzag motion of DTMB5415 ship.

Although the last two statements are only applicable for DTMB5415 ship, it is considered that they are valid for TPTR ships in general. However, more research is needed to support these statements. An additional subsection was devoted to the effects of linear derivatives on maneuvering indices. It was found that there was no linear relationship between the linear derivatives and maneuvering indices.

Currently, MANSIM does not consider external disturbances. Effects of wind, wave and current are also to be included into the software. Future studies can also add quadratic model to the code, which is only working with cubic model in the current form. Furthermore, 3-DOF MMG model will be expanded to a 4-DOF model that includes roll-coupled effects.

Acknowledgements

This study is a part of PhD thesis of the first author, under progress at Istanbul Technical University. First author also would like to thank Mrs. Hulya Sukas for helping with design and general layout of MANSIM.

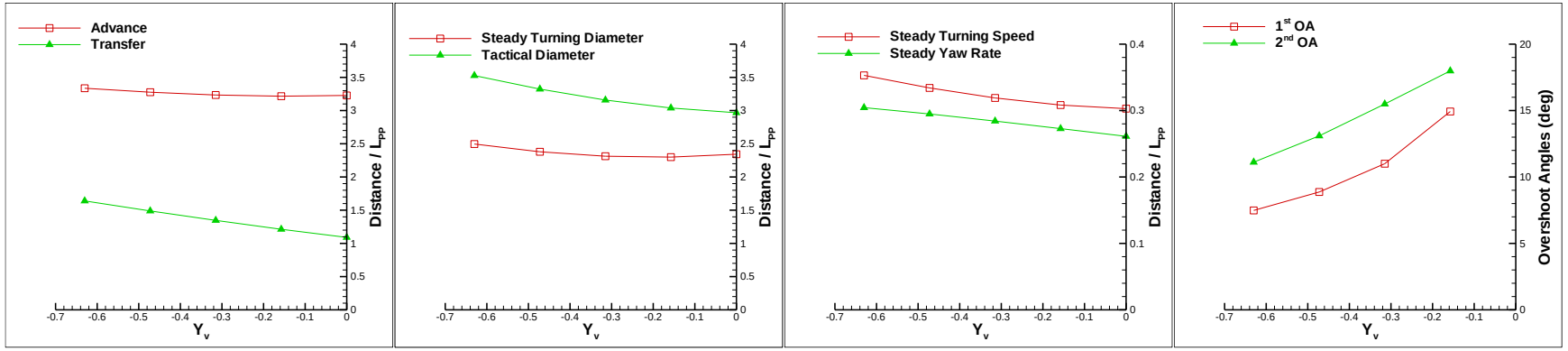

(a) (b) (c) (d)

Figure 14. Effect of Y_v on the behavior of turning circle test indices (a) through (c). On zigzag test (d).

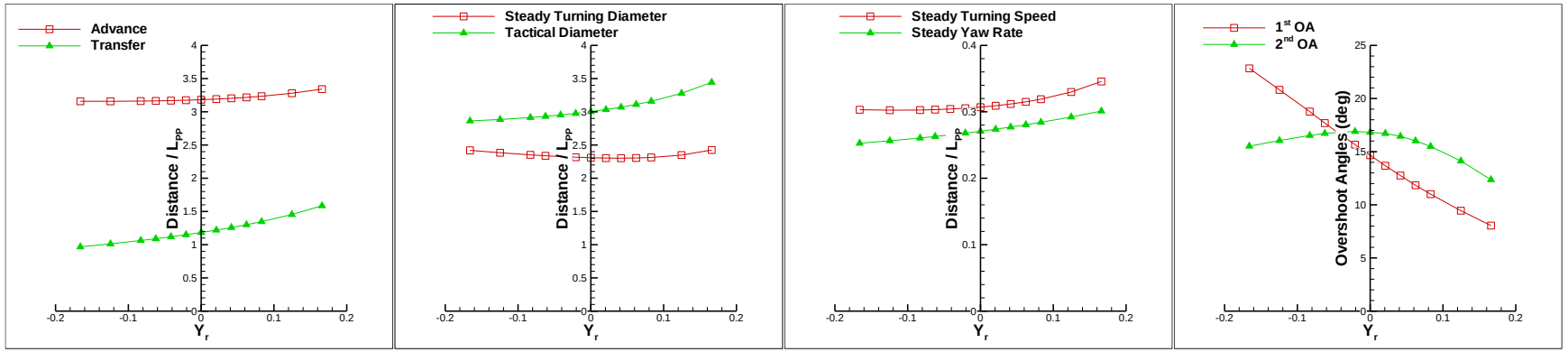

(a) (b) (c) (d)

Figure 15. Effect of Y_r on the behavior of turning circle test indices (a) through (c). On zigzag test (d).

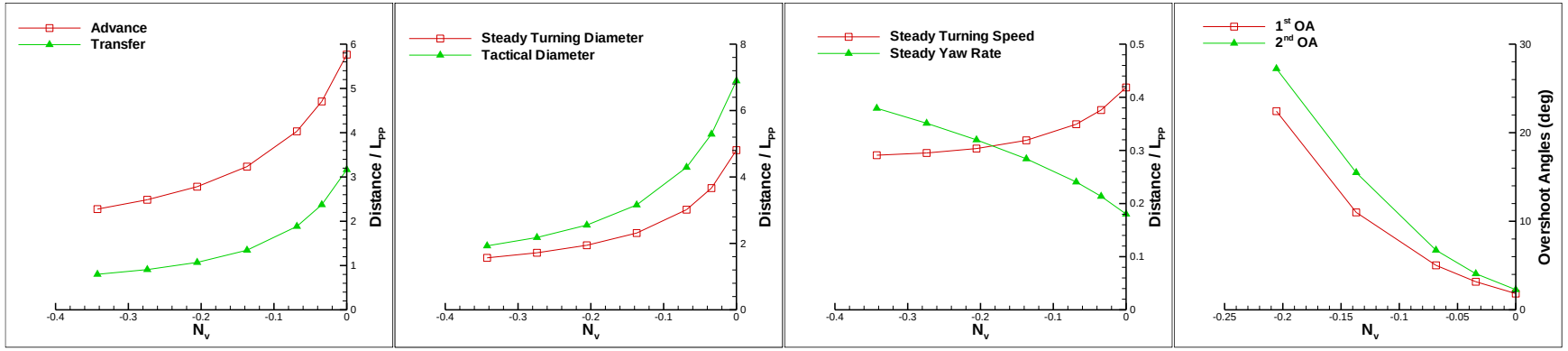

(a) (b) (c) (d)

Figure 16. Effect of N_v on the behavior of turning circle test indices (a) through (c). On zigzag test (d).

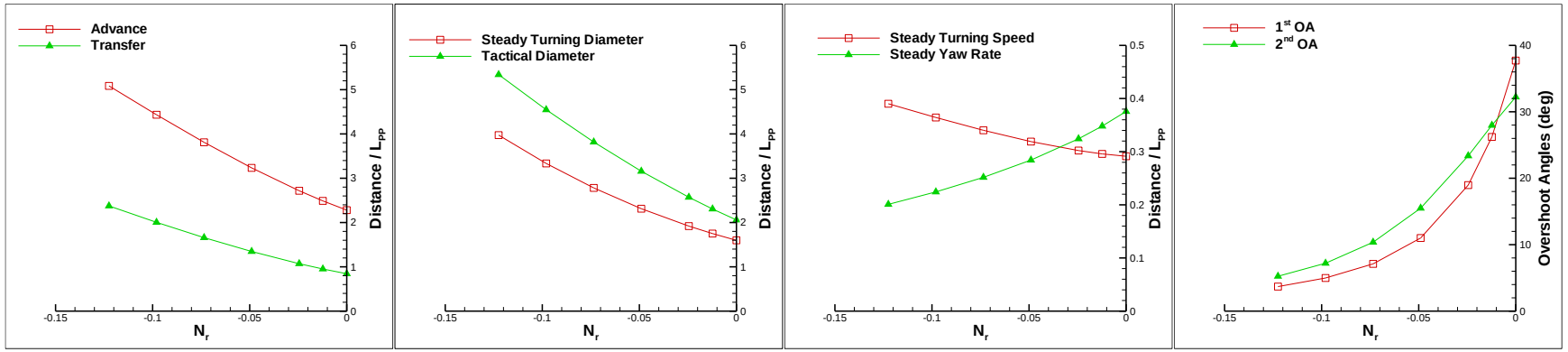

(a) (b) (c) (d)

Figure 17. Effect of N_r on the behavior of turning circle test indices (a) through (c). On zigzag test (d).

References

1. Aoki, I., Kijima, K., Furukawa, Y., Nakiri, Y., 2006. On the prediction method for maneuverability of a full scale ship, Journal of the Japan Soc of Nav. Archic. and Ocean Eng., 3, 157-165.
2. Bhushan, S., Xing, T., Carrica, P., Stern, F., 2009. Model and full-Scale URANS simulations of Athena resistance, powering, seakeeping, and 5415 maneuvering. Journal of Ship Research, 53, 4, 179-198.
3. Broglia, R., Dubbioso, G., Durante, D., Di Mascio, A., 2015. Turning ability analysis of a fully appended twin screw vessel by CFD. Part 1: Single rudder configuration. Ocean Engineering, 105, 275-286.
4. Carrica, P.M., Ismail, F., Hyman, M., Bhushan, S., Stern, F., 2013. Turn and zigzag maneuvers of a surface combatant using a URANS approach with dynamic overset grids. Journal of Marine Science and Technology, 18, 166-181.
5. Clarke, D., Gedling, P., Hine, G., 1983. Application of manoeuvring criteria in hull design using linear theory, Trans. R. Inst. Nav. Archit. 125, 45–68.
6. Cura-Hochbaum, A., 2011. On the numerical prediction of ship's manoeuvring behaviour. Ship Science and Technology, 5, 27-39.
7. Duman, S., Bal, S., 2017. Prediction of the turning and zig-zag maneuvering performance of a surface combatant with URANS. Ocean Systems Engineering-An International Journal, 7, 4, 435-460.
8. Duman, S., Bal, S., 2019. A quick-responding technique for parameters of turning maneuver. Ocean Engineering, 179, 189-201.
9. Fang, M.C., Luo, J.H., Lee, M.L., 2005. A nonlinear mathematical model for ship turning circle simulation in waves. Journal of Ship Research, 49, 2, 69-79.
10. Fujii, H., Tuda, T., 1961. Experimental research on rudder performance (2). J Soc Naval Archit Jpn 110, 31–42 (in Japanese).
11. Guo, H.P., Zou, Z.J., 2017. System-based investigation on 4-DOF ship maneuvering with hydrodynamic derivatives determined by RANS simulation of captive model tests. Applied Ocean Research, 68, 11-25.
12. Harvald, S.A., 1983. Resistance and Propulsion of Ships. John Wiley & Sons.
13. He, S., Kellett, P., Yuan, Z., Incecik, A., Turan, O., Boulougouris, E., 2016. Maneuvering prediction based of CFD generated derivatives. Journal of Hydrodynamics, 28, 2, 284-292.
14. Inoue, S., Hirano, M., ve Kijima, K., 1981. Hydrodynamic derivatives on ship manoeuvring, International Shipbuilding Progress, Vol. 28, No. 321, May.
15. ITTC – Recommended Procedures and Guidelines, 2014. 7.5-02-06-02 rev. 04, Captive Model Test Procedure.

16. Jian-Chuan, Y., Zao-Jian, Z., Feng, X., 2015. Parametric identification of Abkowitz model for ship maneuvering motion by using partial least square regression. Journal of Offshore Mechanics and Arctic Engineering, 137, 3, 031302-031302-7.

17. Kang, D., Nagarajan, V., Hasegawa, K., Sano, M., 2008. Mathematical model of single-propeller twin-rudder ship. Journal of Marine Science and Technology, 13, 207-222.

18. Khanfir, S., Hasegawa, K., Nagarajan, V., Shouji, K., Lee, S. K., 2011. Manoeuvring characteristics of twin-rudder systems: rudder-hull interaction effect on the manoeuvrability of twin-rudder ships, Journal of Marine Science and Technology, 16, 4, 472-490.

19. Khattab, O., 1984. Multiple regression analyses of the hydrodynamic derivatives for maneuvering equations. BSRA Report, W1090, December.

20. Kijima, K., Katsuno, T., Nakiri, Y., Furukawa, Y., 1990. On the maneuvering performance of a ship with the parameter of loading condition, J. Soc. Nav. Archit. Jpn., 168, 141–148.

21. Kinaci, O. K., Gokce, M. K., Alkan, A. D., Kukner, A., 2018. On Self-Propulsion Assessment of Marine Vehicles. Brodogradnja, 69, 4, 29-51.

22. Kinaci, O. K., Sukas, O. F., Bal, S., 2016. Prediction of wave resistance by Reynolds-Averaged Navier-Stokes based computational fluid dynamics approach. Journal of Engineering for the Maritime Environment, 230, 3, 531-548.

23. Kulczyk, J., 1995. Propeller-hull interaction in inland navigation vessel. Trans. Built Environ., 11, 73–89.

24. Lee, H. Y., Shin, S. S., Yum, D. J.,1998. Improvement of Prediction Technique of the Ship's Maneuverability at Initial Design Stage, J Soc Naval Archit Korea, 35, 46-53 (in Japanese).

25. Lee, H.Y., Shin, S.S., 1998. The prediction of ship's manoeuvring performance in initial design stage, Practical Design of Ships and Mobile Units, 633–639.

26. Liu, J., Hekkenberg, R., Quadvlieg, F., Hopman, H., Zhao, B., 2017. An integrated empirical manoeuvring model for inland vessels. Ocean Engineering, 137, 287-308.

27. Liu, J., Quadvlieg, F., Hekkenberg, R., 2016. Impacts of the rudder profile on maneuvering performance of ships. Ocean Enginering, 124, 226-240.

28. Lyster, C. A. , Knights, H. L., 1979. Prediction Equations for Ships' Turning Circles. Trans. NECIES, 95, 217-232.

29. Norrbin, N.H., 1970. Theory and observation on the use of a mathematical mode for ship maneuvering in deep and conned waters. In: Proceedings of the 8th Symposium on Naval Hydrodynamics. Pasadena, CA, 807–904.

30. Obreja, D., Nabergoj, R., Crudu, L., Pacuraru-Popoiu, S., 2010. Identification of hydrodynamic coefficients for maneuvering simulation model of a fishing vessel. Ocean Engineering, 37, 678-687.

31. Ohashi, K., Kobayashi, H., Hino, T., 2018. Numerical simulation of the free-running of a ship using the propeller model and dynamic overset grid method. Ship Technology Research, 65, 3, 153-162.

32. Quadvlieg, F., 2013. Theoretische Berekening van Simulatie modellen voor Binnenvaartschepen ten Behoeve van Maatgevende Manoeuvres (in Dutch). Tech.rep., Maritime Research Institute Netherlands (MARIN), Wageningen, The Netherlands.

33. Sakamoto, N., Carrica, P.M., Stern, F., 2012. URANS simulations of static and dynamic maneuvering for surface combatant: Part 1. Verification and validation for forces, moment, and hydrodynamic derivatives. Journal of Marine Science and Technology, 17, 4, 422-445.

34. Sen, D., 2000. A study on sensitivity of maneuverability performance on the hydrodynamic coefficients for submerged bodies. Journal of Ship Research, 44, 186–196.

35. Smitt, W.L., 1971. Steering and Manoeuvring Full Scale and Model Tests (Parts-2), European Shipbuilding, 20, 1.

36. Sukas, O.F., Kinaci, O.K., Bal, S., 2019. System-based prediction of maneuvering performance of twin-propeller and twin-rudder ship using a modular mathematical model. Applied Ocean Research, 84, 145-162.

37. Sukas, O.F., Kinaci, O.K., Bal, S., 2017a. A review on prediction of ship maneuvering performance, part 1. GMO Journal of Ship and Marine Technology, 210, 37–75 (In Turkish).

38. Sukas, O.F., Kinaci, O.K., Bal, S., 2017b. A review on prediction of ship maneuvering performance, part 2. GMO Journal of Ship and Marine Technology, 210, 76–105 (In Turkish).

39. Sutulo, S., Soares, C.G., 2014. An algorithm for offline identification of ship maneuvering mathematical models from free-running tests. Ocean Engineering, 79, 10-25.

40. Toxopeus, S., Sadat-Hosseini, H., Visonneau, M., Guilmineau, E., Yen, T.G., Lin, W.M., Grigoropoulos, G., Stern, F., 2018. CFD, potential flow and system-based simulations of fully appended free running 5415M in calm water and waves. International Ship Building Progress, 65, 227-256.

41. Xu, H., Vassani, H., Soares, C.G, 2019. Uncertainty analysisof the hydrodynamic coefficients estimation of a nonlinear manoeuvring model based on planar motion mechanism tests. Ocean Engineering, 173, 450-459.

42. Yasukawa, H., Sakuno, R., Yoshimura, Y., 2019. Practical maneuvering simulation method of ships considering the roll-coupled effect. Journal of Marine Science and Technology, https://doi.org/10.1007/s00773-019-00625-4.

43. Yasukawa, H., Yoshimura, Y., 2015. Introduction of MMG standard method for ship maneuvering predictions, Journal of Marine Science and Technology, 20, 37-52.

44. Yoon, H., Simonsen, C.D., Benedetti, L., Longo, J., Toda, Y., Stern, F., 2015. Benchmark CFD validation data for surface combatant 5415 in PMM maneuvers-Part 1: Force/moment/motion measurements. Ocean Engineering, 109, 705-734.

45. Yoshimura, Y., Masumoto, Y., 2012. Hydrodynamic database and maneuvering prediction method with medium high-speed merchant ships and fishing vessels. In: International Conference on Marine Simulation and Ship Maneuverability (MARSIM'12). Singapore. Apr.

46. Zhang, C., Liu, X., Wan, D., Wang, J., 2019. Experimental and numerical investigations of advancing speed effects on hydrodynamic derivatives in MMG model, part 1: X_{vv}, Y_v, N_v. Ocean Engineering, 179, 67-75.

47. Zhang, X.G., Zou, Z.J., 2013. Estimation of the hydrodynamic coefficients from captive model test results by using support vector machines. Ocean Engineering, 73, 25-31.

48. Zhou, Z., Yan, S., Feng, W., 1983. Manoeuvring prediction of multiple-purpose cargo ships (in Chinese), Ship Eng., 6, 21–36.